4-30-2021

UVC disinfection of COVID-19 and associated bacteria on personal protective equipment

Ryden Christopher Smith

UVC disinfection of COVID-19 and associated bacteria on personal protective equipment

By

Ryden Christopher Smith

Approved by:

Wilburn Whittington (Major Professor)
Hongjoo Rhee
Haitham El Kadiri
Yucheng Liu (Graduate Coordinator)
Jason M. Keith (Dean, Bagley College of Engineering)

A Thesis
Submitted to the Faculty of
Mississippi State University
in Partial Fulfillment of the Requirements
for the Degree of Master of Science
in Mechanical Engineering
in the Department of Mechanical Engineering

Mississippi State, Mississippi

April 2021

Name: Ryden Christopher Smith

Date of Degree: April 30, 2021

Institution: Mississippi State University

Major Field: Mechanical Engineering

Major Professor: Wilburn Whittington

Title of Study: UVC disinfection of COVID-19 and associated bacteria on personal protective equipment

Pages in Study: 69

Candidate for Degree of Master of Science

The COVID-19 pandemic has been an unprecedented public health crisis around the world and has created novel needs in the healthcare industry. Primary among these needs is a vast shortage in personal protective equipment (PPE) such as masks and gloves. This is problematic due to the near constant of COVID-19 cases in hospitals around the United States. In an effort to meet the need for more PPE, new disinfection techniques must be found to "recycle" used PPE. UVC light has previously been used by healthcare facilities for years to disinfect surfaces such as stainless steel and are frequently used in operating room sterilization and dentist offices. UVC light's effectiveness on porous materials such as masks has not been substantially investigated prior to the COVID-19 pandemic. This work shows the effectiveness and efficiency of UVC disinfection on porous surfaces for the COVID-19 virus and other bacteria.

Key words: COVID-19, Coronavirus, Pandemic, Ultraviolet Light, UVC, Disinfection, UVC Testing, Corona Killer

DEDICATION

To the Lord, my beautiful Fiancé, Jordan, and my family. Thank you for your love and support of me pursuing my dreams.

ACKNOWLEDGEMENTS

I would like to thank all those at the Center for Advanced Vehicular Systems (CAVS) for all your time, training, and support. Dr. Wilburn Whittington led me and our team with an infectious passion and vigor for life, and, in doing so, became one of my dear friends. My research team, Trey Leonard, Jennie Maddox, Billy Zhang, Aidan Duncan, Marouane Jarachi and Justin Easley thank you for providing a family for me here. To Dr. Keun Seok Seo and the MSD design team without whom this work would not have been completed. To Andrea Oakley, Jennifer Carruth, and Elaine Turner, thank you for making all our research possible. To Melissa Mott, Robert Malley, Steve Murray, and Michael Newman, thank you for teaching me all the equipment at CAVS, and for your kind patience as I learned. Lastly, a sincere thank you to all the other faculty and graduate students who helped me reach my goals here at Mississippi State.

TABLE OF CONTENTS

LIST OF TABLES

LIST OF FIGURES

CHAPTER I

INTRODUCTION

1.1 Filtering Facepiece Respirators and Disinfection Techniques

Leading into the discussion of disinfection and the work performed in this paper, the question arises – what is disinfection, and how is disinfection related to two other words, cleaning and sanitizing, which are frequently used in association with the COVID-19. Cleaning is a method by which dust and debris is removed by scrubbing or washing. Whereas sanitizing is a reduction of certain bacteria as specified by the sanitizing agent by a measurable amount. Lastly, disinfection is the destruction or inactivation of both the bacteria and viruses in their entirety [1]. Out of the personal protective equipment used to defend healthcare workers from COVID-19, the most important is the N95 filtering facepiece respirator (FFR). There are other FFRs than the N95, but the N95 is the gold standard because it filters 95% of particulates at 0.3 micron [2].

Ever since the FFR N95 became ubiquitous in the healthcare industry, many have been looking at the effect an influenza pandemic could have on FFR N95 supplies from as early as the 1990s to the present day [3]–[8]. Consequently, many began to look at various disinfection methods by which supplies of single FFRs could be extended beyond their normal life span [9]–[17]. Some of the disinfection methods investigated are, microwave-generated steam, microwave oven radiation, warm moist heat, Ultraviolet light (both UVA and UVC), ethylene oxide (EtO), vaporized hydrogen peroxide (VHP), ethanol, sodium hypochlorite, bleach, and others.

FFRs are unique from other equipment in healthcare where disinfection occurs because they are porous filters, so many of the typical disinfection guidelines cannot apply. As such, the following are the most important concerns when it comes to any form of disinfection of FFRs. Maximum disinfection of any viruses or bacteria must occur; the integrity of the FFR must be preserved; the filtering function of the FFR must be preserved, and a proper seal with the wearer must be maintained. If these four criteria are met, then the disinfection method can be considered effective [3].

1.2 UVC Compared Other Disinfection Methods

UVC also known as UVGI (Ultraviolet Germicidal Irradiation) is light with a 254 nm wavelength which has a deleterious effect on virus and bacteria [18]. Single Strand RNA (ssRNA) viruses are particularly susceptible to UVC and can be inactivated to 99% viral reduction by a UVC does of 2.64 to 6.40 mJ/cm^2 [19]. The following sections compare UVC to other available forms of disinfection currently in literature and elucidate why UVC was preferable for this study.

1.2.1 Moist Heat and Microwave-Generated Steam and Radiation

Using a conventional household microwave to disinfect FFRs is an attractive idea because of the ready availability around the nation [5]. Microwaves function by supplying a radio frequency to that which is being microwaved. This action excites water molecules specifically which generates heat. Microwaves have been shown to have lethal effects on bacteria [20]. The radiation of microwaves combined with the steam from the necessary water reservoir in this method result in an effective method for disinfection in terms of the viability of viruses and bacteria. Similar to the microwave, an oven with a larger of reservoir of water can

also be used for disinfection in the form of moist heat. Table 1.1 shows the comparison of UVC to microwave-generated steam (MGS) and moist heat (MH) for two FFRs. It can be seen that while the biocidal effects of the MGS and MH method are effective, both methods negatively affect the filtration performance of the FFRs when compared with UVC.

Table 1.1 Mean Penetration (n=5) of 1% NaCl Aerosol at 300-nm Particle Size (Lore et al., 2012)

FFR	Control	UVGI	MGS	MH
1860s (%)	1.08	0.99	1.51	1.04
1870 (%)	0.39	0.37	0.99	0.99

1.2.2 Ethylene Oxide and Vaporized Hydrogen Peroxide

When disinfecting FFRs with ethylene oxide (EtO), there is an EtO exposure time followed by a set time of aeration. The aeration process is to remove any residual EtO residue on the FFR before use once more. Cycle times can vary, but typically one cycle takes five hours with one hour for EtO exposure and four hours for aeration. Vaporized hydrogen peroxide (VHP) is similar in process to the EtO method. With this method, the FFRs are exposed to the VHP gas for a time and then left to aerate. The total cycle time is shorter than that of the EtO method, however cellulose-based objects such as cotton absorb hydrogen peroxide which can lead to two issues [15]. One, the hydrogen peroxide concentration does not get high enough to achieve disinfection within the FFR, and, two, residual hydrogen peroxide can be left on the FFRs which needs off-gassing before use.

1.2.3 Ethanol and Bleach

Ethanol and bleach disinfection follow similar procedures to one another. First the ethanol or bleach mixture is added to the N95 FFR via a pipette. Then the saturated FFR is dried in a biosafety cabinet for ten minutes. The disinfection process with the ethanol was found to have a relative survival rate of bacteria of over 20% making it ineffective when compared to other methods [12]. The bleach did achieve 99% disinfection, however the smell of bleach remained on the FFRs even after further drying. Residual bleach and hypochlorite powder can have both irritating and corrosive effects on human's skin, eyes, and respiratory tract which makes bleach an unsafe method disinfection.

1.3 UVC Disinfection Advantages and Potential

From the studies prior to this work, it was found that EtO, VHP, and UVC were the three leading methods of disinfection which adhered to the four criteria for successful disinfection. However, the primary concern of the VHP and EtO methods is the throughput of the disinfection. Specifically, how well the disinfection agent penetrates the full thickness of the FFR to yield complete disinfection. This is not a concern for UVC as much because it has been shown to penetrate the thicknesses of FFR materials. There have been many studies on UVC and its disinfection capabilities dating as far back as the 1970s [21]–[30]. UVC equipped biosafety cabinets are one method by which disinfection has been evaluated as they are prevalent in healthcare facilities. Additionally, Nebraska Medicine [27] published a study detailing how a UVC light room can be constructed in order to disinfect N95 FFRs for reuse.

The primary advantages of UVC above other methods for disinfection from the perspective of implementation is that UVC lighting solutions are affordable and scalable. From the view of the four criteria by which disinfection can be considered effective, UVC also is met

with success. UVC has been shown to have minimal effect on particle penetration and flow resistance of FFRs as shown in Figure 1.1 by Lindsley. Additionally, since UV-C is light and not a liquid disinfectant, there is no off-gassing or other potential health risks to wearers once disinfected.

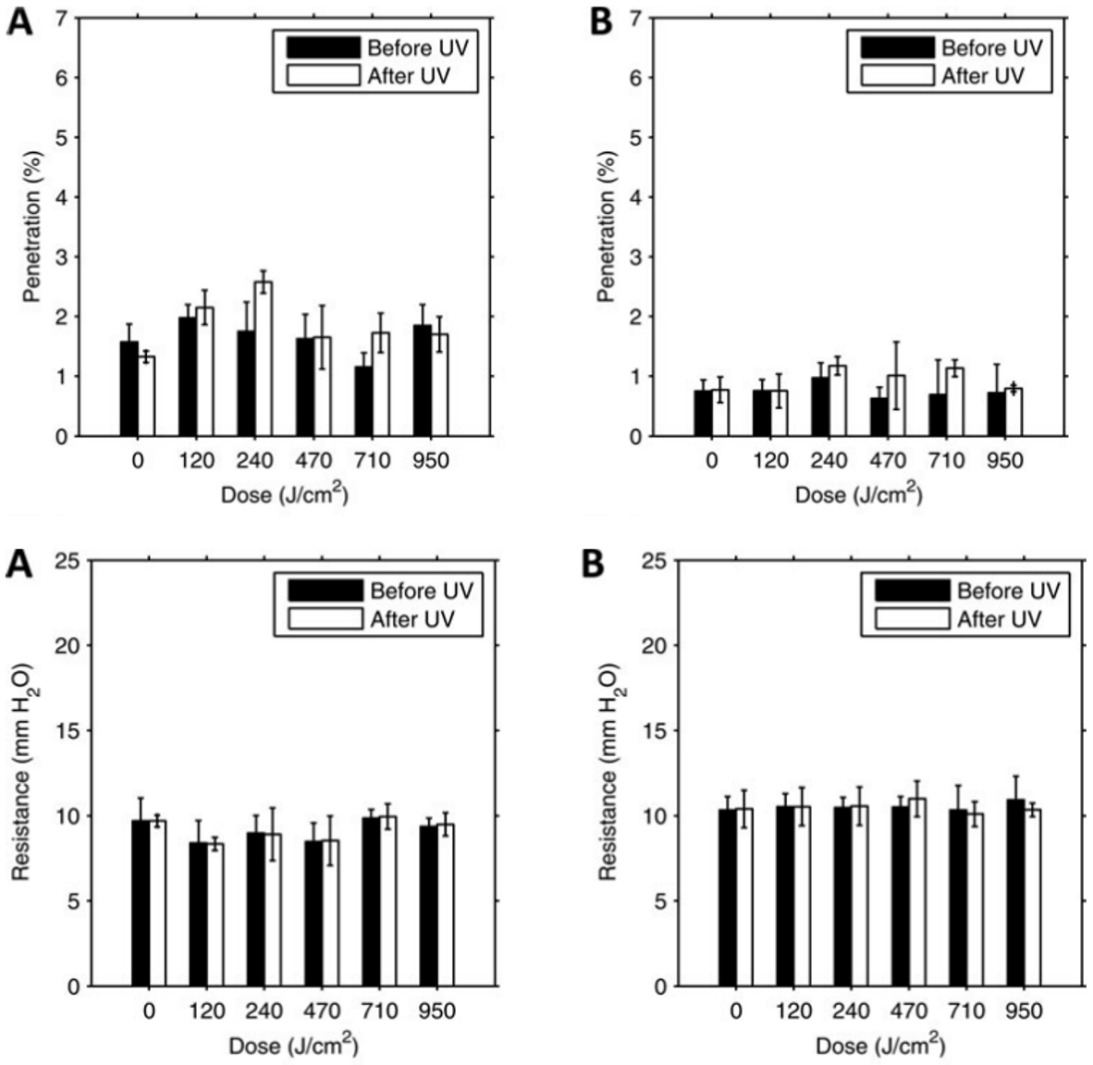

Figure 1.1 Particle penetration and flow resistance vs. UVGI exposure for respirator material (Lindsley et al., 2015)

(A) 3M 1860; (B) 3M 9210. Each pair of bars shows the mean penetration for four 37 mm test coupons before and after UVGI exposure. The units of "mm H_2O" are used by convention; 1 mm H_2O = 9.8 N/m^2. Error bars show the standard deviation.

The primary drawback to UVC is the potential for the UVC to damage the FFR structure or straps which directly influence how effective of a seal a FFR can have [31]–[33]. From Lindsley's study it was found that as the UVC dose (in J/cm^2) increased, the burst strength of the FFR material decreased by up to 99%, and the breaking strength of the straps decreased by up to 23% for both 3M N95 FFRs. These decreases in strength would render UVC as a meaningful option for disinfection a last resort. However, the lowest dose considered by Lindsley's work is 120 J/cm^2, and the lowest dose required for complete ssRNA inactivation is 6.40 mJ/cm^2 as shown by Tseng and Li. Following the trend of FFR strength in Lindsley's study, decreasing the dosage by a large factor would dramatically increase the amount of disinfection cycles a FFR could take before its filtration and fitment performance were negatively affected, rendering UVC a very effective disinfection method.

1.4 UVC Disinfection of FFRs from COVID-19

In light of the COVID-19 pandemic, there is a need now more than ever to lighten the burden on N95 FFR supplies. Disinfection and reuse of FFRs could increase the life of each FFR by 5 times or more, artificially increasing the available supply. While work has been done in the realm of UVC to find the inactivation doses for bacteria and other viruses like H1N1, there is not a clear consensus on what dosage of UVC it takes to entirely inactivate COVID-19. Typically for ssRNAs, a dosage of 6.40 mJ/cm^2 achieves 99% inactivation on hard surfaces [19]. The work by Nebraska Medicine in their design of their disinfection room specified a dosage of 60 mJ/cm^2, 10 times that of the dosage needed on hard surfaces, to account for the porosity of the N95 FFRs. Viscusi's work utilized a dosage of 180 mJ/cm^2 to analyze the effect of UVC on N95 FFRs undergoing disinfection, and Mills' work utilized 1 J/cm^2 on H1N1. Consequently, there is not a

clear dosage of UVC for the disinfection of COVID-19 in N95 FFRs. This study seeks to fill that gap.

CHAPTER II

THE UVC DISINFECTION CHAMBER

2.1 The Design of the UVC Disinfection Chamber

In March of 2020, a need was made apparent to the Department of Mechanical Engineering at Mississippi State University for a method by which to recycle or reuse N95 masks. This method needed to be affordable, portable, and effective in use to be helpful and adoptable by healthcare providers. Consequently, UVC light was selected as the best experimental method to test initially because of its scalability, its ability to work on porous materials, and lack of any liquid medium. The housing selected was a conventional truck toolbox found at any hardware store. Aluminum is one of the few materials that reflects ultraviolet light, so the toolbox being polished aluminum allowed for a better dispersion of light in and around the N95s. The toolbox was modified to have two fluorescent fixtures mounted facing one another to allow the light to hit both sides of the N95 which were placed in the chamber and hung from a wire running the length of the chamber. Figure 2.1 shows the inside and outside of the chamber with the dial timer control and warning light on the lid.

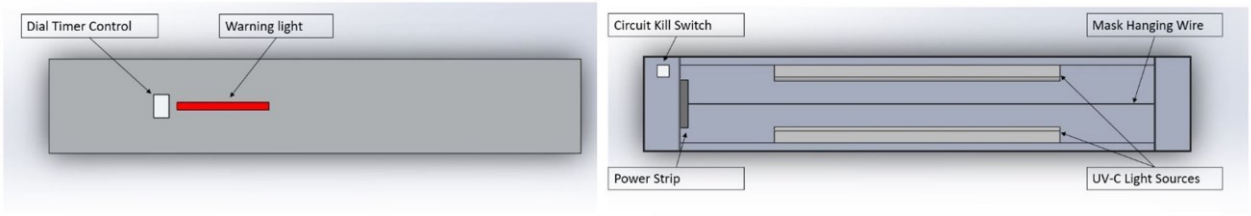

Figure 2.1 Top view of the UVC Disinfection Chamber

The complete summary of how the UVC Disinfection Chamber was constructed can be found in Appendix B. This appendix details the measurements and all the wiring for the chamber's lights and safety measures. Additionally, Appendix A details the operation manual for how to use a completed UVC Disinfection Chamber.

2.2 Initial Testing of the UVC Disinfection Chamber Prototype

Following the prior work out of Nebraska Medicine, a dosage of 60 mJ/cm^2 was designed for the UVC Disinfection Chamber. The UVC lights used in the chamber were G30T8 germicidal bulbs sourced form Sankyo Denki, which has a spectral energy distribution shown in Figure 2.2. This shows that the energy output of the lights used is as a 254 nm wavelength, meaning that there is little energy put toward wavelengths that would not cause virus inactivation.

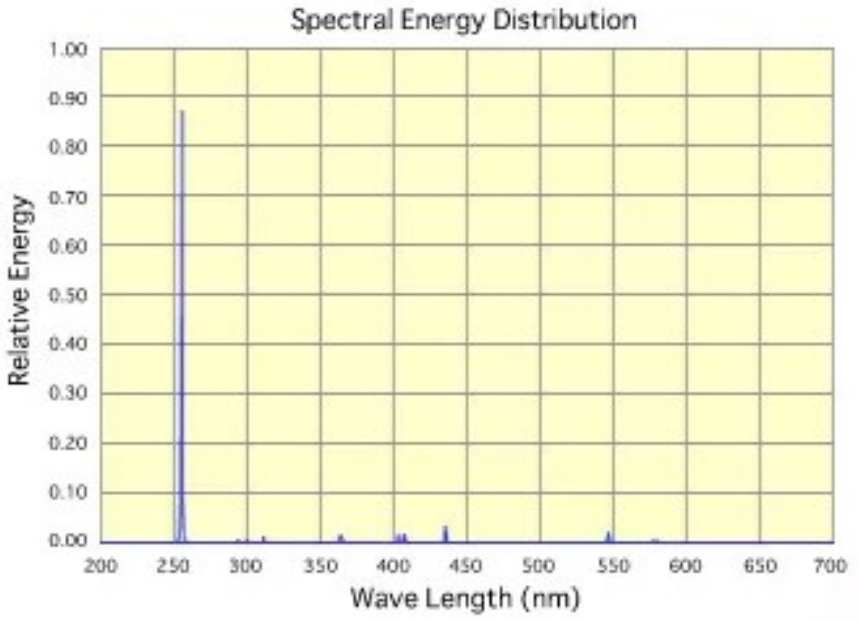

Figure 2.2 Sankyo Denki spectral energy distribution for G30T8 UVC bulbs

To test the power output of the lights once installed in the chamber, a Thor Labs PDA25K2 light sensor was used [34] which produces light measurements in Volts and had a light sensor area of 4.8 mm^2. Figure 2.3 shows the responsivity of this sensor to different wavelengths of light. At 254 nm, the responsivity of the sensor is 0.031 A/W.

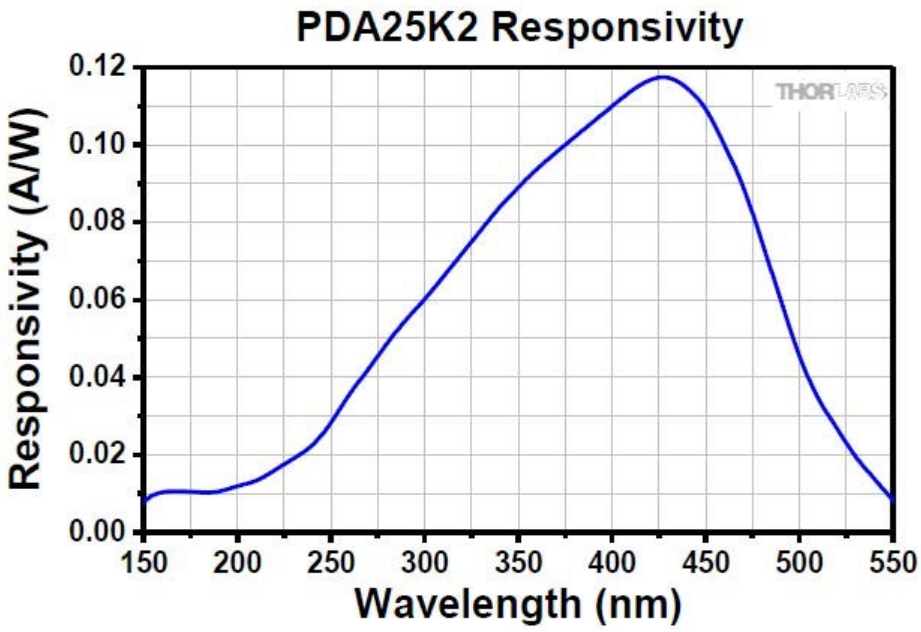

Figure 2.3 Thor Labs PDS25K2 responsivity vs wavelength.

The sensor when set to a gain of 60 dB with a terminal resistance of 50 Ω had an amperage to voltage output of 0.75 x 10^{-6} V/A. The sensor's responsivity at 254 nm and the amperage to voltage output measured combine to form a direct voltage to power relationship which can be directly related to voltage. This factor is 23.25 V/mW.

Utilizing this factor, the dosage desired, 60 mJ/cm^2 and an assumed time, a minimum voltage required was calculated in Equations 2.1-2.3.

$$E = 60\frac{mJ}{cm^2} * 4.8\, mm^2 = 2.88\, mJ \tag{3.1}$$

Where, E is the energy output of the sensor for the prescribed dosage.

$$P = \frac{E}{30\ min} = 0.0016\ mW \tag{3.2}$$

Where, P is the average power output for the prescribed and assumed time of 30 minutes.

Using the average power output and the voltage to power factor found from the light sensor's responsivity, an average voltage output for disinfection can be found. Additionally, it is assumed that of the light measured of by the light sensor, only 75 % of that measurement is UVC.

$$Voltage_{required} = P * 23.25\ \frac{V}{mW} *\ 0.75 = 0.02775\ V \tag{3.3}$$

What Equation 2.3 shows is that if the voltage measured by the light sensor in the UVC disinfection chamber is equal to or greater than 0.02775 V, then the prescribed dosage of 60 mJ/cm^2 has been met, and single-strand RNA like COVID-19 can be assumed to be deactivated.

2.3 UVC Disinfection Chamber Validation Methodology

Using the Thor Labs sensor, the UVC light output from the fluorescent fixtures was measured according to a 32-point inspection process wherein the voltage output was taken at many different locations and orientations. Figure 2.4 shows the eight discrete measurement locations. At each of these locations, four different measurements were taken, two facing each light fixture, and two facing each end of the chamber. Using this measurement test matrix, it was

able to be determined if each light fixture produced an equal amount of UVC dosage at the center of the chamber, and to what level light was reflected around the chamber.

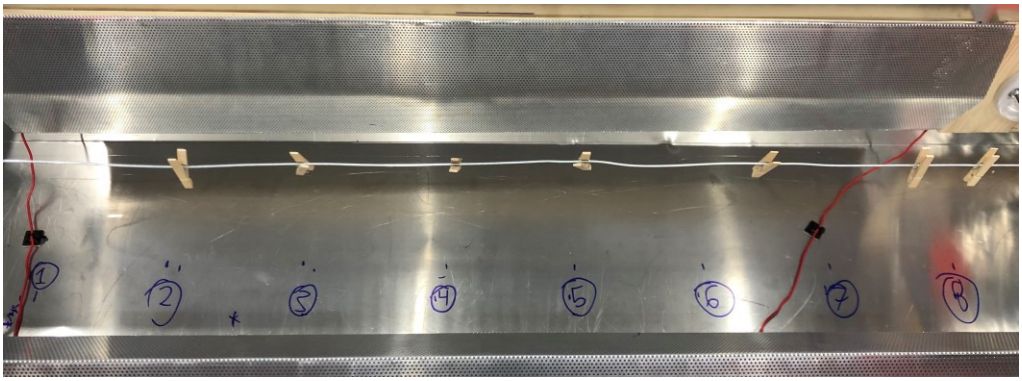

Figure 2.4 The interior of the UVC Disinfection Chamber with the eight measurement locations

In addition to the 32-point test matrix, each location was tested twice more, once with the sensor facing each of the light fixtures. The difference in these measurements is that the light sensor was placed directly behind a dust mask disk so that the sensor was completely covered by the mask disk. This enabled the measurement of the amount of UVC passing through the entirety of the dust mask which is directly related to the dosage amount the inner layers of the mask received. This is shown in Figure 2.5.

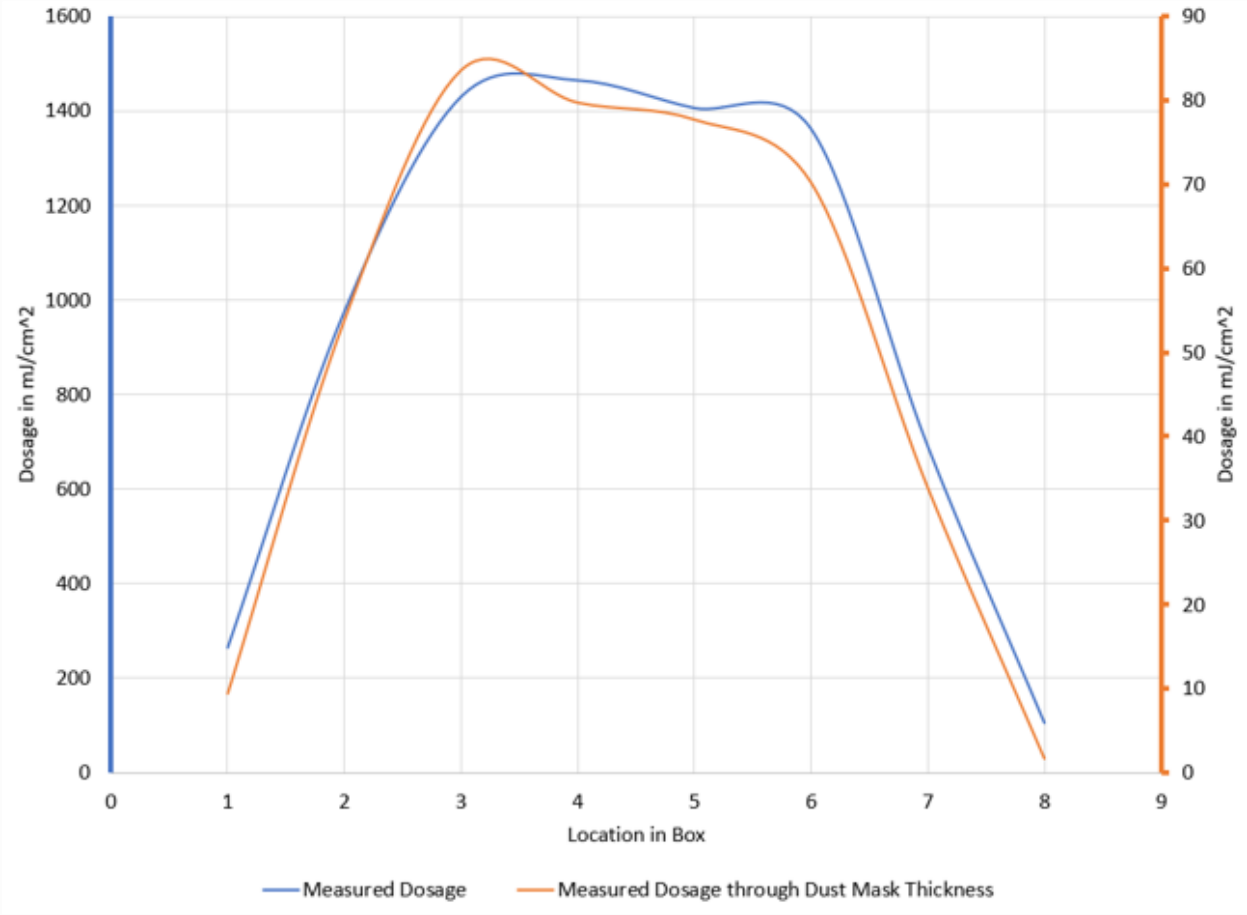

Figure 2.5 The dosage plotted vs mask location for both the measured dosage and the measured dosage through the thickness of the dust mask

A N95 was also tested in a similar manner in the UVC Disinfection Chamber. For this, another eight measurements were taken with the sensor in the between locations 4 and 5, the center of the chamber. The first of these was taken as just the sensor without the n95. This measurement corresponds to number 1 on the x-axis in Figure 2.6. Next, a measurement was taken with the n95 disk completely covering sensor. This corresponded to number 2. Then, one layer of the mask was removed, and a measurement was taken. This process was repeated until the mask was entirely removed, and then one more measurement was taken with no mask covering. These correspond to numbers 3-8 in Figure 2.6.

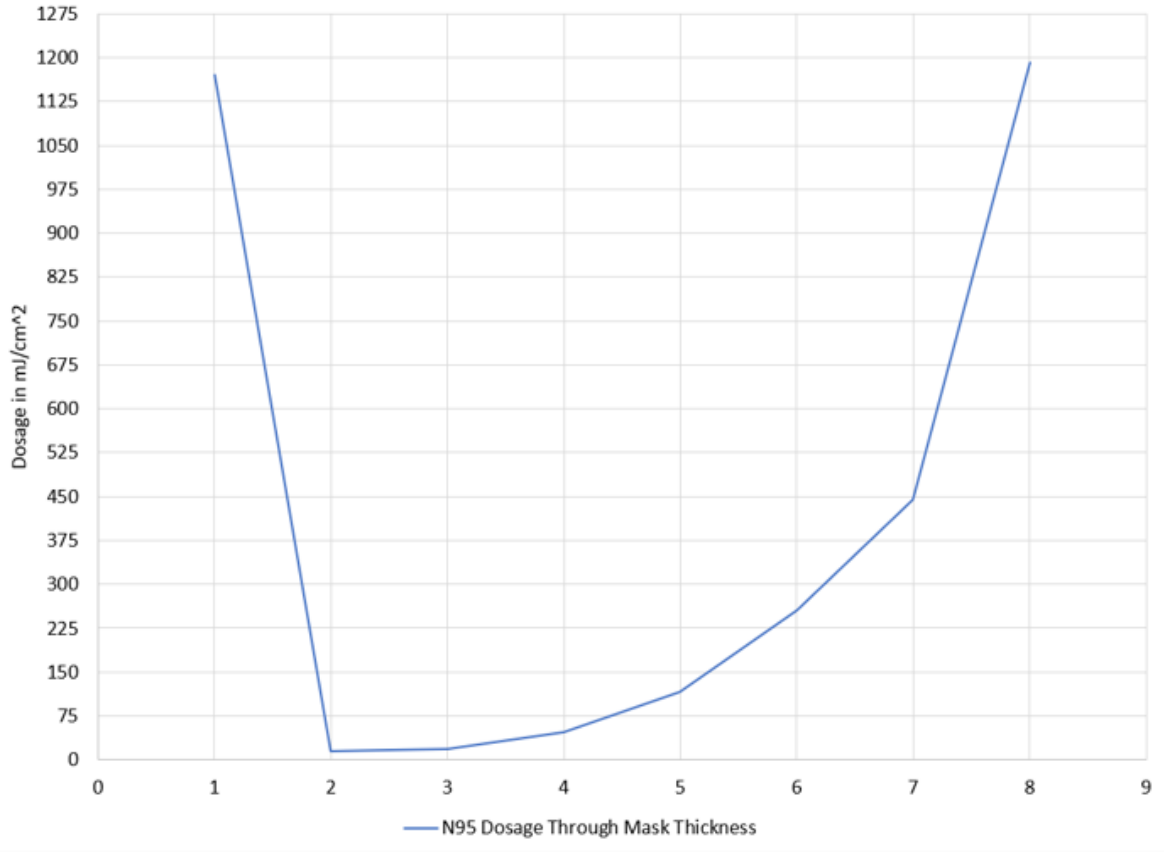

Figure 2.6 Dosage values measured through the N95 as the mask thickness decreases

What was learned from the dosage measurements is as follows. Locations 1 and 8 as seen in Figure 2.4 were unsuitable for any form of mask disinfection. Locations 2 and 7 received adequate UVC dosage to disinfect masks given enough exposure time, and locations 3-6 provided the optimum about of UVC dosage to disinfect masks. The measurements on the N95 showed that when having the N95 between both UVC fixtures, enough light penetrates the mask to disinfect it through its thickness.

2.4 Implementation of UVC Disinfection Chamber

Once constructed and validated, the UVC Disinfection Chamber was adopted by health care providers in and around Starkville, MS ranging as far out as Arkansas. The primary

beneficiaries of the technology were institutions that were smaller than major hospitals, but still had patient populations battling COVID-19 outbreaks. An example was the Mississippi VA, just to the west of Starkville, MS.

CHAPTER III

UVC TESTING ON COVID-19 AND OTHER BACTERIA

Once the UVC Disinfectant chamber was completed, it was sent to the College of Veterinary Medicine at Mississippi State University to test the effectiveness of the chamber on the feline strand Coronavirus, a CDC approved surrogate for COVID-19.

3.1 Antiviral Testing of UVC Disinfection Chamber on PPE

Feline CRFK cell line (ATCC CCL-94) was cultured in Eagle's Minimum Essential Medium supplemented with 10 % fetal bovine serum. Feline infectious peritonitis virus (ATCC VR-1812) was propagated and assayed in the feline CRFK cell line. Briefly, FIPV was infected to 80-90 % confluent monolayer of CRFK cell line and incubated for 3 days to develop cytopathogenic effect (CPE). The cell lysates were centrifuged at 100 x g for 100 minutes to pellet the cell debris. The supernatant containing viruses then was sterilized with a filter (0.45 um). The number of FIPV was titrated by determining TCID50 (tissue culture infectious dose at the 50 % endpoint) as described by Reed and Muench [35]. The minimal detection of FIPV by TCID50 was 5.7 viruses/ml. The viral stocks were then aliquoted and stored at -80 oC.

To determine the efficacy of the PPE disinfectant chamber, 0.1 ml of viral suspension or vehicle control was inoculated onto the medical mask coupon and exposed to UV for a contact time of 15, 30, and 60 minutes. At the conclusion of the contact time, mask coupons were transferred to a microfuge tube containing 1 mL of PBS, and vortexed vigorously to release the viruses. The supernatants were serially diluted in 10 folds and inoculated onto CRFK monolayers

prepared in a 96-well plate in replicates of six per dilutions. In some experiments, a serially diluted supernatant was inoculated onto CRFK cells prepared in a 6-well plate. After viral absorption for 1 hour, supernates were removed and then 0.5 % soft agar in EMEM was overlaid. After 72 hours incubation, a viral plaque formation was determined by 0.3 % crystal violet staining.

3.2 Antibacterial Testing of UVC Disinfection Chamber on PPE

Staphylococcus aureus (ATCC 25923), Enterococcus faecalis (ATCC 51575), Klebsiella pneumoniae (ATCC 35657), and Escherichia coli (ATCC 25922) were obtained from the American Type Culture Collection (ATCC). Bacterial strains were cultured in tryptic soy broth at 37 oC for 18 hours. Bacterial cells were adjusted to 5x107 CFU/ml in PBS and 50 uL of bacterial suspension was inoculated onto mask coupons and exposed to the PPE disinfectant chamber UVC for a contact time of 5 and 15 minutes. At the conclusion of the contact time, mask coupons were transferred to a microfuge tube containing 1 mL of PBS, and vortexed vigorously to release the bacteria. The supernatants were serially diluted in 10 folds and inoculated onto tryptic soy agar (TSA) in replicates of six per dilutions. The plates were incubated at 37 oC for 24 h for qualitative evaluation of bacteria inactivation.

3.3 Results of Antiviral Effect of UVC Disinfection on PPE

As shown in Table 3.1, FIPV was rapidly inactivated by the UVC disinfection chamber. The reduction was greater than 5.56 logs within a contact time of 5 minutes. A plaque formation assay also clearly supported the inactivation of FIPV by UV (Figure 1). Without exposure to UV, FIPV produced a clear PPE which was completely inhibited after exposure to UV within 5 minutes.

Table 3.1 Inactivation of FIPV by UVC Disinfection Chamber

TCID90										
	Contact Time (min)	Count 1	Count 2	Count 3	Count 4	Count 5	Count 6	Mean	SD	Log 10 Reduction
No UV	0	358,000	364,000	344,000	361,000	398,000	358,000	363,833	18,093	N/A
UV	5	<5.7	<5.7	<5.7	<5.7	<5.7	<5.7	N/A	N/A	>5.56
	10	<5.7	<5.7	<5.7	<5.7	<5.7	<5.7	N/A	N/A	>5.56
	15	<5.7	<5.7	<5.7	<5.7	<5.7	<5.7	N/A	N/A	>5.56
	30	<5.7	<5.7	<5.7	<5.7	<5.7	<5.7	N/A	N/A	>5.56

Seen in Figure 3.1 a mask coupon was inoculated with 10 uL of FIPV (5×108 pfu/ml), followed by exposure in the UVC disinfection chamber for 5 to 30 min. After UVC exposure, coupons were vigorously vortexed in PBS and inoculated onto the mono layer of CFRK cells. After viral absorption for 1 hour, supernates were removed and then 0.5 % soft agar in EMEM was overlaid. After 72 hours incubation, a viral plaque formation indicated by a clear zone was determined by 0.3 % crystal violet staining.

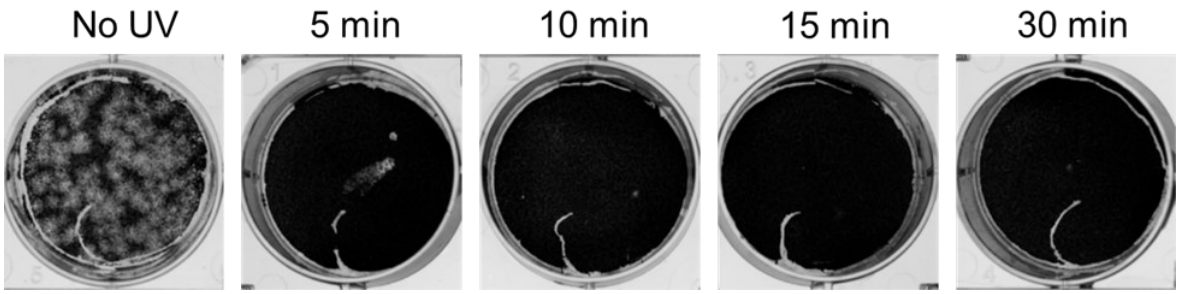

Figure 3.1 UVC Effect on FIPV Shown with Crystal Violet Staining

3.4 Results of Antibacterial Testing of UVC Disinfection on PPE

After exposure to the UVC disinfection chamber for 5 minutes, all bacterial strains were inactivated within a range of 2.89 to 4.05 logs. After exposure to the PPE disinfectant chamber

UVC for 15 minutes, all bacterial strains were completely inactivated. These results are shown in Table 3.2 - Table 3.5. Figure 3.2 shows graphically the effect of UVC on COIVD-19.

Table 3.2 Inactivation of *Staphylococcus aureus* by UVC disinfection chamber

	Contact Time (min)	Count 1	Count 2	Count 3	Count 4	Count 5	Count 6	Mean	SD	Log 10 Reduction
No UV	0	2,570,000	2,200,000	2,980,000	2,410,000	2,540,000	2,410,000	2,518,333	261,183	N/A
UV	5	0	0	1000	0	2000	500	583	801	3.64
	15	0	0	0	0	0	0	0	0	>6.40

Table 3.3 Inactivation of Vancomycin resistant *Enterococcus faccalis* by UVC disinfection chamber

	Contact Time (min)	Count 1	Count 2	Count 3	Count 4	Count 5	Count 6	Mean	SD	Log 10 Reduction
No UV	0	2,650,000	2,540,000	2,530,000	2,150,000	2,680,000	2,190,000	2,456,667	230,101	N/A
UV	5	0	0	1000	0	200	100	217	392	4.05
	15	0	0	0	0	0	0	0	0	>6.39

Table 3.4 Inactivation of *Escherichia coli* by UVC disinfection chamber

	Contact Time (min)	Count 1	Count 2	Count 3	Count 4	Count 5	Count 6	Mean	SD	Log 10 Reduction
No UV	0	2,250,000	2,350,000	2,450,000	2,470,000	2,630,000	2,540,000	2,448,333	134,821	N/A
UV	5	2000	1000	1200	0	0	0	700	837	3.54
	15	0	0	0	0	0	0	0	0	>6.39

Table 3.5 Inactivation of *Klebsiella pneumoniae* by UVC disinfection chamber

	Contact Time (min)	Count 1	Count 2	Count 3	Count 4	Count 5	Count 6	Mean	SD	Log 10 Reduction
No UV	0	2,240,000	2,890,000	2,050,000	2,100,000	2,320,000	2,100,000	2,283,333	313,985	N/A
UV	5	1000	0	200	0	0	0	200	400	2.89
	15	0	0	0	0	0	0	0	0	>5.50

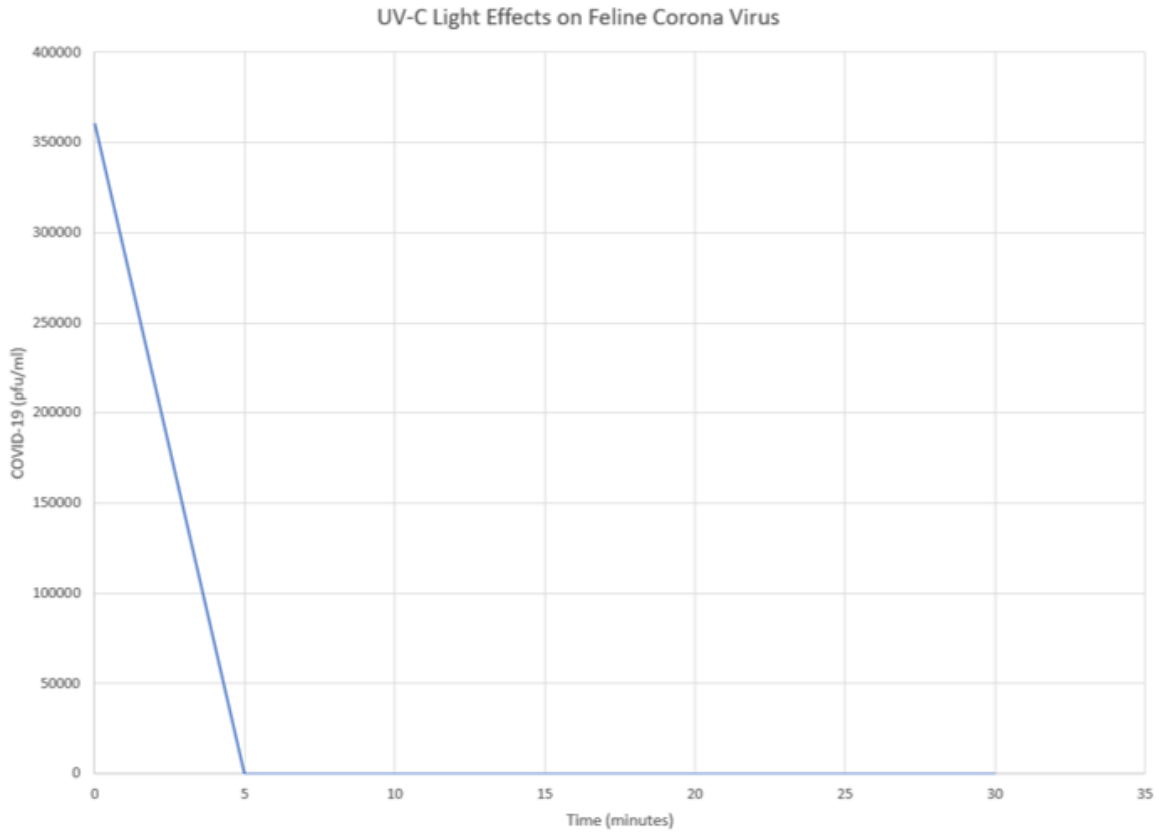

Figure 3.2 The effects of UVC on the COVID-19 virus population as time increases

CHAPTER IV

UVC DISINFECTION CHAMBER SCALABILITY

This work primarily focuses on the UVC Disinfection Chamber itself, however, an additional smaller study was also performed on the potential for scalability in the design. Specifically, a design was considered in which the chamber itself was removed, and the UVC lights were held by a portable tower, thus allowing the lights to be brought into rooms to disinfect the room itself.

4.1 Design of the UVC Disinfection Tower

The design for the UVC Disinfection Tower came as a natural progression from the UVC Disinfection Chamber and had the primary advantage of reducing the time required to disinfect a room which frequently must be done in all healthcare providers facilities [36], [37]. Additionally, this technology could allow for a higher disinfection efficiency as each surface hit by the UVC would be disinfected, removing any potential for missing areas with conventional methods.

Similar in concept to the UVC Disinfection Chamber, the UVC Disinfection Tower was designed to be as simple and affordable in construction as possible. The base consisted of a repurposed speaker stand tripod which allowed for height adjustability while maintaining strength. Mounted to the tripod was a prefabricated sheet metal junction box, which contained the wiring harness and battery pack. On the face of the junction box, a prefabricated REL Inc., profusion LED UVC light was mounted. The prototype is shown in Figure 4.1.

Figure 4.1 Completed UVC Disinfection Tower prototype design

4.2 Initial Testing of the UVC Disinfection Tower Prototype

The testing for the UVC Disinfection Tower used a different light sensor than the testing performed on the UVC Disinfection Chamber. This new sensor, a Linshang LS125 UV Meter, allowed for dosage in mJ/cm^2 to be measured directly along with the irradiance value. The irradiance of the light was then used in conjunction with the desired dosage to directly calculate the time required for disinfection in this light. Equation 4.1 shows the inverse square law which was used to calculate the irradiance given a known irradiance at a known distance.

$$I_2 = I_1(\frac{x_2}{x_1})^2 \quad (5.1)$$

Where,

I_2 = calculated irradiance at distance x_2, $\mu W/cm^2$

I_1 = known irradiance at distance x_1, $\mu W/cm^2$

x_2 = distance from light source, in

x_1 = distance from light source, in

For calculating the irradiance when the UVC light had an angle of incidence greater than zero, Lambert's cosine law was used, and is shown in Equation 4.2.

$$I_3 = I_2 * \cos(\alpha) \quad (5.2)$$

Where,

I_3 = Irradiance corrected for angle of incidence, $\mu W/cm^2$

α = Angle of incidence, rad

Lastly, the time required to disinfect a surface could be found by dividing the required dosage by the calculated irradiance value. This is shown in Equation 4.3.

$$time_{disinfection} = \frac{D}{I_3} \quad (5.3)$$

Where,

D = Dosage required, mJ/cm^2

Using these three equations, the desired dosage of 5 mJ/cm^2, and the Linshang LS125 UV meter, the time required for disinfection at various working distances was able to be calculated for the UVC Disinfection Tower. Six different distances were tested with two of the six distance tested with varying incidence angles. The time to disinfect was then calculated from the measurements taken.

4.3 Results of the UVC Disinfection Tower

From the results of the FIPV inactivation study in the and the equations presented in Chapter II, it can be surmised that the required dosage for the inactivation of COVID-19 by the UVC light requires a dosage around 5 mJ/cm^2. Using the lower dosage amount, the time to disinfect was calculated for the UVC Disinfection Tower and is shown in Table 4.1.

Table 4.1 Disinfection Time for UVC Disinfection Tower at Varying Working Distances

Angle (deg)	Distance (in)	UVC Irradiance Calculated	UVC Irradiance Tested	Time
0	2	2166	2098.4	2.38 s
45	2	1531.6	1530	3.27 s
0	15	38.5	37.8	2.20 min
45	15	27.2	30	2.78 min
0	62	1.9	1.9	43.86 min
0	86	1.2	1.1	1.26 hr
0	96	0.9	0.6	2.31 hr
0	120	0.6	0.1	13.89 hr

Irradiance values are in μW/cm^2

It can be seen in Table 4.1 that for more practical distances, the UVC light source tested takes too long to disinfect to be considered a viable alternative to conventional methods available. However, the light unit tested was designed to be used in an array of identical lights

linked together. Additionally, a linear relationship between irradiance and number of lights can be assumed. Consequently, if two stands were used with ten of the UVC lights each, the below disinfection times in Table 4.2 could be achieved.

Table 4.2 Disinfection Time for Updated UVC Disinfection Towers at Varying Working Distances

Angle (deg)	Distance (in)	UVC Irradiance Tested	UVC Irradiance Total	Time
0	2	2098.4	41,968	0.12 s
45	2	1530	30,600	0.16 s
0	15	37.8	756	6.61 s
45	15	30	600	8.33 s
0	62	1.9	38	2.19 min
0	86	1.1	22	3.79 min
0	96	0.6	12	6.94 min
0	120	0.1	2	41.67 min

Irradiance values are in $\mu W/cm^2$

The time required for disinfection shown in Table 4.2 is much more practical, but still not entirely ideal as each room turnover would take just under forty-five minutes. As such, two more stands could be used, for a total of four, one for each corner of a conventional room which would allow a complete room disinfection time of under thirty minutes. Alternatively, if more powerful UVC lights were used in each stand, such as the bulbs used in the UVC disinfection chamber, the turn-around time for disinfecting a room would drop to almost nothing, making the UVC Disinfection Tower a viable method by which to disinfect rooms.

CHAPTER V

CONCLUSIONS AND FUTURE WORK

5.1 Conclusions

In conclusion, the UVC disinfection technology is unequivocally viable for disinfection of the Coronavirus and multiple types of bacteria. It has negligible effects on N95 FFR flow resistance and filtration capability. While it does cause wear on masks, it increases the life cycle of N95 FFRs by five times or more. The advantages provided by this technology cannot be overstated. If the process of UVC disinfection of N95 FFRs had been more developed in its capability before the COVID-19 pandemic, then the N95 FFR shortage might have been much less severe for healthcare workers around the world.

Additionally, the capability of this technology allows for great flexibility and expandability to disinfect more than just FFRs through the use of the UVC disinfection tower or a device similar. Though UVC can cause skin and eye irritation in humans, UVC still could provide a meaningful way to turn over patient or public rooms during off hours. Specifically, the use of UVC to disinfect rooms could mitigate fluctuations in disinfection quality sometimes found in conventional disinfection methods.

5.2 Future Work

Moving forward, the primary area of investigation is in the development of the UVC Disinfection Tower. While there is great promise, simply scaling the number of REL lights in each array could become cost prohibitive for most institutions looking to use this technology. A more cost-effective method for increasing the irradiance output of each stand needs to be found to make the towers competitive with the conventional methods available.

REFERENCES

[1] "Clorox." https://www.clorox.com/resources/coronavirus/whats-the-difference-between-cleaning-sanitizing-and-disinfecting/#:~:text=Know the Difference. 1 Cleaning removes dust, debris,(like influenza and rhinovirus) on hard, nonporous surfaces.

[2] S. A. National Institute for Communicable Diseases, "Frequently Asked Questions KAINOS + Frequently Asked Questions," no. 1099, pp. 1–3, 2019, [Online]. Available: https://www.nicd.ac.za/diseases-a-z-index/covid-19/frequently-asked-questions/.

[3] D. Farsi, M. Mofidi, B. Mahshidfar, and P. Hafezimoghadam, "Consider the Options; Can Decontamination and Reuse be the Answer to N95 Respirator Shortage in COVID-19 Pandemic?," *Adv. J. Emerg. Med.*, vol. 4, no. 2s, pp. e41–e41, 2020, doi: 10.22114/ajem.v0i0.378.

[4] B. K. Heimbuch *et al.*, "A pandemic influenza preparedness study: Use of energetic methods to decontaminate filtering facepiece respirators contaminated with H1N1 aerosols and droplets," *Am. J. Infect. Control*, vol. 39, no. 1, pp. e1–e9, 2011, doi: 10.1016/j.ajic.2010.07.004.

[5] M. B. Lore, B. K. Heimbuch, T. L. Brown, J. D. Wander, and S. H. Hinrichs, "Effectiveness of three decontamination treatments against influenza virus applied to filtering facepiece respirators," *Ann. Occup. Hyg.*, vol. 56, no. 1, pp. 92–101, 2012, doi: 10.1093/annhyg/mer054.

[6] D. Nogee and A. J. Tomassoni, "Covid-19 and the N95 respirator shortage: Closing the gap," *Infect. Control Hosp. Epidemiol.*, vol. 41, no. 8, p. 958, 2020, doi: 10.1017/ice.2020.124.

[7] D. Rempel, "Scientific Collaboration During the COVID-19 Pandemic: N95DECON.org," *Ann. Work Expo. Heal.*, vol. 64, no. 8, pp. 775–777, 2020, doi: 10.1093/annweh/wxaa057.

[8] S. Srinivasan, "N95 filtering facepiece respirators during the COVID-19 pandemic: Basics, types, and shortage solutions," *Malaysian Orthop. J.*, vol. 14, no. 2, pp. 1–7, 2020, doi: 10.5704/MOJ.2007.002.

[9] D. W. M. Gardner and G. Shama, "Modeling UV-induced inactivation of microorganisms on surfaces," *J. Food Prot.*, vol. 63, no. 1, pp. 63–70, 2000, doi: 10.4315/0362-028X-63.1.63.

[10] S. Lehmann *et al.*, "New hospital disinfection processes for both conventional and prion infectious agents compatible with thermosensitive medical equipment," *J. Hosp. Infect.*, vol. 72, no. 4, pp. 342–350, 2009, doi: 10.1016/j.jhin.2009.03.024.

[11] E. Fisher, S. Rengasamy, D. Viscusi, E. Vo, and R. Shaffer, "Development of a test system to apply virus-containing particles to filtering facepiece respirators for the evaluation of decontamination procedures," *Appl. Environ. Microbiol.*, vol. 75, no. 6, pp. 1500–1507, 2009, doi: 10.1128/AEM.01653-08.

[12] T. H. Lin, F. . Tang, P. C. Hung, Z. C. Hua, and C. Y. Lai, "Relative survival of bacillus subtilis spores loaded on filtering facepiece respirators after five decontamination methods," doi: 10.1111/ina.12475.

[13] T. H. Lin, C. C. Chen, S. H. Huang, C. W. Kuo, C. Y. Lai, and W. Y. Lin, "Filter quality of electret masks in filtering 14.6–594 nm aerosol particles: Effects of five decontamination methods," *PLoS One*, vol. 12, no. 10, pp. 1–15, 2017, doi: 10.1371/journal.pone.0186217.

[14] G. V. K. Rastogi, "Relevant to Medical Treatment Facilities with Ultraviolet C Light," vol. 172, no. August, pp. 1166–1169, 2007.

[15] D. J. Viscusi, M. S. Bergman, B. C. Eimer, and R. E. Shaffer, "Evaluation of five decontamination methods for filtering facepiece respirators," *Ann. Occup. Hyg.*, vol. 53, no. 8, pp. 815–827, 2009, doi: 10.1093/annhyg/mep070.

[16] E. Vo, S. Rengasamy, and R. Shaffer, "Development of a test system to evaluate procedures for decontamination of respirators containing viral droplets," *Appl. Environ. Microbiol.*, vol. 75, no. 23, pp. 7303–7309, 2009, doi: 10.1128/AEM.00799-09.

[17] J. Van Loon *et al.*, "Reuse of filtering facepiece respirators in the COVID-19 era," *Sustain.*, vol. 13, no. 2, pp. 1–20, 2021, doi: 10.3390/su13020797.

[18] W. Kowalski, *Ultraviolet Germical Irradiation*, vol. 53, no. 9. 2009.

[19] C. C. Tseng and C. S. Li, "Inactivation of viruses on surfaces by ultraviolet germicidal irradiation," *J. Occup. Environ. Hyg.*, vol. 4, no. 6, pp. 400–405, 2007, doi: 10.1080/15459620701329012.

[20] S. Gedikli, Ö. Tabak, Ö. Tomsuk, and A. Cabuk, "Effect of Microwaves on Some Gram Negative and Gram Positive Bacteria," *J. Appl. Biol. Sci.*, vol. 2, no. 1, pp. 67–71, 2008.

[21] J. . Card *et al.*, "UV Sterilization of Personal Protective Equipment with Idle Laboratory Biosafety Cabinets During the Covid-19 Pandemic," *medRxiv*, pp. 1–17, 2020.

[22] M. Dulęba-Majek, “Transmission of UV radiation through woven fabrics in dependence on the inter-thread spaces,” *Fibres Text. East. Eur.*, vol. 73, no. 2, pp. 34–38, 2009.

[23] E. M. Fisher and R. E. Shaffer, “A method to determine the available UV-C dose for the decontamination of filtering facepiece respirators,” *J. Appl. Microbiol.*, vol. 110, no. 1, pp. 287–295, 2011, doi: 10.1111/j.1365-2672.2010.04881.x.

[24] A. Patond and R. Narang, “A low cost ingenious approach for ultraviolet decontamination of N95 filtering face-piece respirators to deal with dwindling supply during the COVID-19 pandemic,” *J. Mahatma Gandhi Inst. Med. Sci.*, vol. 25, no. 2, p. 80, 2020, doi: 10.4103/jmgims.jmgims_48_20.

[25] W. H. Glaze, G. R. Peyton, S. Lin, R. Y. Huang, and J. L. Burleson, “Destruction of Pollutants in Water with Ozone in Combination with Ultraviolet Radiation. 2. Natural Trihalomethane Precursors,” *Environ. Sci. Technol.*, vol. 16, no. 8, pp. 454–458, 1982, doi: 10.1021/es00102a005.

[26] E. L. Gorsuch, S. A. Grinshpun, K. Willeke, T. Reponen, C. E. Moss, and P. A. Jensen, “Method for evaluating germicidal ultraviolet inactivation of biocontaminated surfaces,” *Int. J. Occup. Saf. Ergon.*, vol. 4, no. 3, pp. 287–297, 1998, doi: 10.1080/10803548.1998.11076395.

[27] J. J. Lowe *et al.*, “N95 Filtering Facepiece Respirator Ultraviolet Germicidal Irradiation (UVGI) Process for Decontamination and Reuse,” 2020, [Online]. Available: https://www.nebraskamed.com/sites/default/files/documents/covid-19/n-95-decon-process.pdf.

[28] Q. S. Meng and C. P. Gerba, “Comparative inactivation of enteric adenoviruses, poliovirus and coliphages by ultraviolet irradiation,” *Water Res.*, vol. 30, no. 11, pp. 2665–2668, 1996, doi: 10.1016/S0043-1354(96)00179-0.

[29] D. Mills, D. A. Harnish, C. Lawrence, M. Sandoval-Powers, and B. K. Heimbuch, “Ultraviolet germicidal irradiation of influenza-contaminated N95 filtering facepiece respirators,” *Am. J. Infect. Control*, vol. 46, no. 7, pp. e49–e55, 2018, doi: 10.1016/j.ajic.2018.02.018.

[30] D. Sylvain and L. Tapp, “UV-C Exposure and Health Effects in Surgical Suite Personnel,” *Heal. Hazard Eval. Rep.*, no. May, 2009, [Online]. Available: http://www.cdc.gov/niosh/hhe/reports/pdfs/2007-0257-3082.pdf.

[31] A. Kilic, E. Shim, and B. Pourdeyhimi, “Electrostatic Capture Efficiency Enhancement of Polypropylene Electret Filters with Barium Titanate,” *Aerosol Sci. Technol.*, vol. 49, no. 8, pp. 666–673, 2015, doi: 10.1080/02786826.2015.1061649.

[32] N. E. Bopp, D. H. Bouyer, C. M. Gibbs, J. E. Nichols, C. A. Ntiforo, and M. A. Grimaldo, "Multicycle Autoclave Decontamination of N95 Filtering Facepiece Respirators," *Appl. Biosaf.*, vol. 25, no. 3, pp. 150–156, 2020, doi: 10.1177/1535676020924171.

[33] W. G. Lindsley *et al.*, "Effects of Ultraviolet Germicidal Irradiation (UVGI) on N95 Respirator Filtration Performance and Structural Integrity," *J. Occup. Environ. Hyg.*, vol. 12, no. 8, pp. 509–517, 2015, doi: 10.1080/15459624.2015.1018518.

[34] "PDA25K2 GaP Switchable Gain Detector User Guide," [Online]. Available: https://www.thorlabs.com/drawings/41f568c8ac1f3c9a-BBDA8469-0FE0-F89F-034E78A0FB2FF41F/PDA25K2-Manual.pdf.

[35] L. J. Reed and H. Muench, "A Simple Method of Estimating Fifty per Cent Endpoints," *J. Epidemiol.*, vol. 27, no. 3, pp. 493–497, 1938, [Online]. Available: https://doi.org/10.1093/oxfordjournals.aje.a118408.

[36] J. M. Boyce, N. L. Havill, D. G. Dumigan, M. Golebiewski, O. Balogun, and R. Rizvani, "Monitoring the Effectiveness of Hospital Cleaning Practices by Use of an Adenosine Triphosphate Bioluminescence Assay," *Infect. Control Hosp. Epidemiol.*, vol. 30, no. 7, pp. 678–684, 2009, doi: 10.1086/598243.

[37] A. G. Buchan, L. Yang, and K. D. Atkinson, "Predicting airborne coronavirus inactivation by far-UVC in populated rooms using a high-fidelity coupled radiation-CFD model," *Sci. Rep.*, vol. 10, no. 1, pp. 1–7, 2020, doi: 10.1038/s41598-020-76597-y.

APPENDIX A

UVC DISINFECTION CHAMBER OPERATING MANUAL

OPERATIONAL MANUAL

1. Don personal protective equipment (PPE) in the form of a clean mask and gloves.
2. Press either of the two silver buttons on opposing sides of the chamber to release the latch, then lift in the center of the lid to open the chamber. If the chamber is powered on when the lid opens it will turn off automatically.
3. Remove the soiled PPE mask from the storage bag, and, using clothes pins, hang the mask by the strap, close to the mask body.
4. Ensure that the mask is hanging parallel in between the two UVC light emitting fixtures such that the front of the mask faces one of the fixtures while the back of the mask faces the opposite fixture.
5. When all the masks for the cycle are hung, push down in the center of the lid, denoted by a white rectangle, until the latch clicks closed.
6. Turn the dial timer on the lid of the chamber to 10 minutes – the orange LED light on the lid will turn on indicating that the disinfection process is taking place.
7. While the UVC disinfection chamber is working, sanitize all the touch points on the box, denoted by the white lines, and the dial timer.
8. When the timer dings, the disinfection process is complete.
9. Don new PPE gloves, and press either of the two silver buttons on opposing sides of the chamber to release the latch, then lift the center of the lift to open the chamber.
10. Remove the disinfected masks one at a time, placing each into the appropriate clean container for transport.
11. Repeat this procedure as many times as necessary.

APPENDIX B

UVC DISINFECTION CHAMBER CONTRUCTION AND INSTALLATION MANUAL

Table B.1 UVC Disinfection Chamber Tools Required for Assembly

Number	Tool Name:
1	Hand Drill
2	Level
3	File
4	Stepper Drill Bits
5	Screwdriver
6	Ratchet Set (English)
7	Wrench Set (English)
8	Alan Wrenches (English)
9	Wire Cutters
10	Pliers
11	Sheet Metal Brake (Optional)
12	Sheet Metal Shears (Optional
13	Circular Saw
14	Label Maker (Optional)

Table B.2 Bill of Materials for Construction

Quantity	Part	Vendor	Vendor Part Number	Price
1	Aluminum Toolbox	Lowes	1053446	309.00
1	16 Gauge Power Cable	Lowes	74527	8.98
1	Electrical Tape	Lowes	39340	1.99
1	Wire Nuts	Lowes	48615	3.18
1	15ft Power Strip	Lowes	101418	23.98
1	LED Strip Light	Lowes	877634	14.98
1	15A Contact Switch	Lowes	543142	6.66
1	RACO Internal Switch Box	Lowes	70967	0.99
1	RACO Internal Switch Box Cover	Lowes	19846	0.98
1	Tork 1-hour timer	Lowes	871316	17.98
1	External Switch Box	Lowes	1437916	8.96
1	J-Hook Pack	Lowes	1087594	14.98
2	Tow Handles	Lowes	803447	9.16
2	Casters	Lowes	169308	8.36
1	Orange Fluorescent Paint	Lowes	416297	5.28
1	White Duct Tape	Lowes	156887	6.98
1	Zip-ties	Lowes	757003	13.88
3	Zip-tie Holders	Lowes	292685	7.14
1	Hanging Wire	Lowes	62947	4.58
1	Masking Tape	Lowes	590693	3.98
4	Large Rubber Grommets	Lowes	139378	5.44
1	Small Rubber Grommet	Lowes	139357	1.45
1	Rigid Comp Connector	Lowes	76986	6.38
1	Sheet of Perforated Aluminum	McMaster-Carr	9232T141	63.13
1	1/4” x 2” Bolt Pack	McMaster-Carr	90044A125	8.42
1	1/4” x 1-1/2” Bolt Pack	McMaster-Carr	90044A123	13.25
1	1/4” Lock Nut Pack	McMaster-Carr	95615A120	4.39
1	10-32 x 1/2” Bolt Pack	McMaster-Carr	91251A342	10.07
1	10-32 x 1” Bolt Pack	McMaster-Carr	91251A347	8.85
1	10-32 Lock Nut Pack	McMaster-Carr	90631A411	3.35
1	Clothes Pins	McMaster-Carr	12275T53	8.32
1	10-24 x 1” Bolt Pack	McMaster-Carr	91251A242	11.19
1	10-24 Lock Nut Pack	McMaster-Carr	90631A011	3.31
1	1/4” x 1/2” Bolt Pack	McMaster-Carr	91251A537	11.38
1	Aluminum 6061 Flat Bar	McMaster-Carr	8975K196	3.03
1	Crimp Spade Connector Pack	McMaster-Carr	7060K67	15.04
2	G30T8 Sankyo Denki Bulbs	Atlanta Light Bulbs	RM-0392 3000635	30.12
1	Workhorse 5 Ballast	Atlanta Light Bulbs	WH5-120-L FULHAM	25.49
2	36” Fluorescent Fixture	Home Depot	1000974698	47.62
Total				**752.25**

CONSTRUCTION MANUAL

1. Layout all the tools and parts listed in the tools list and bill of materials as seen in Figure B.1.

Figure B.1 Tools and parts necessary for UVC Disinfection Chamber Construction

2. Remove the Craftsman logo from the front center of the toolbox and remove the stickers from inside the lid.
3. Using the masking tape, tape off the LED strip light such that everything except the actual light itself is taped.
4. Then, use the orange, fluorescent paint to paint the light of the LED strip light. The completed strip light is shown in Figure B.2.

Figure B.2 The painted LED strip light

5. Once the LED strip light is painted, measure 6” from the front edge of the lid and 10-3/4” from the left-hand edge of the lid. Make a corner mark with a sharpie for the external switch box.
6. Measure 1/2” to the right of the rightmost edge of the external switch box and make a mark. Next, center the width of the LED strip light perpendicular to the length of the external switch box.
7. The two J-hooks need to be in a line with each other and parallel to the external switch box. Thus, measure 3” to the left of the external switch box and make a mark. This mark is the centerline for the two J-hooks.
8. Then, measure 4-1/2” from the front edge of the toolbox and make a mark. This mark is for the back edge of the first J-hook. Now measure an additional 9-1/4” from that mark. That is the mark for the back edge of the second J-hook.
9. With the J-hooks placed according to the steps above, mark the mount holes on the lid for both J-hooks, the LED strip light, and the external switch box.

10. Next, drill seven holes through the lid for each of the mount holes that were marked in step 9 with the hand drill and a stepper drill bit. The layout of these four parts and the drill holes are shown in Figure B.3.

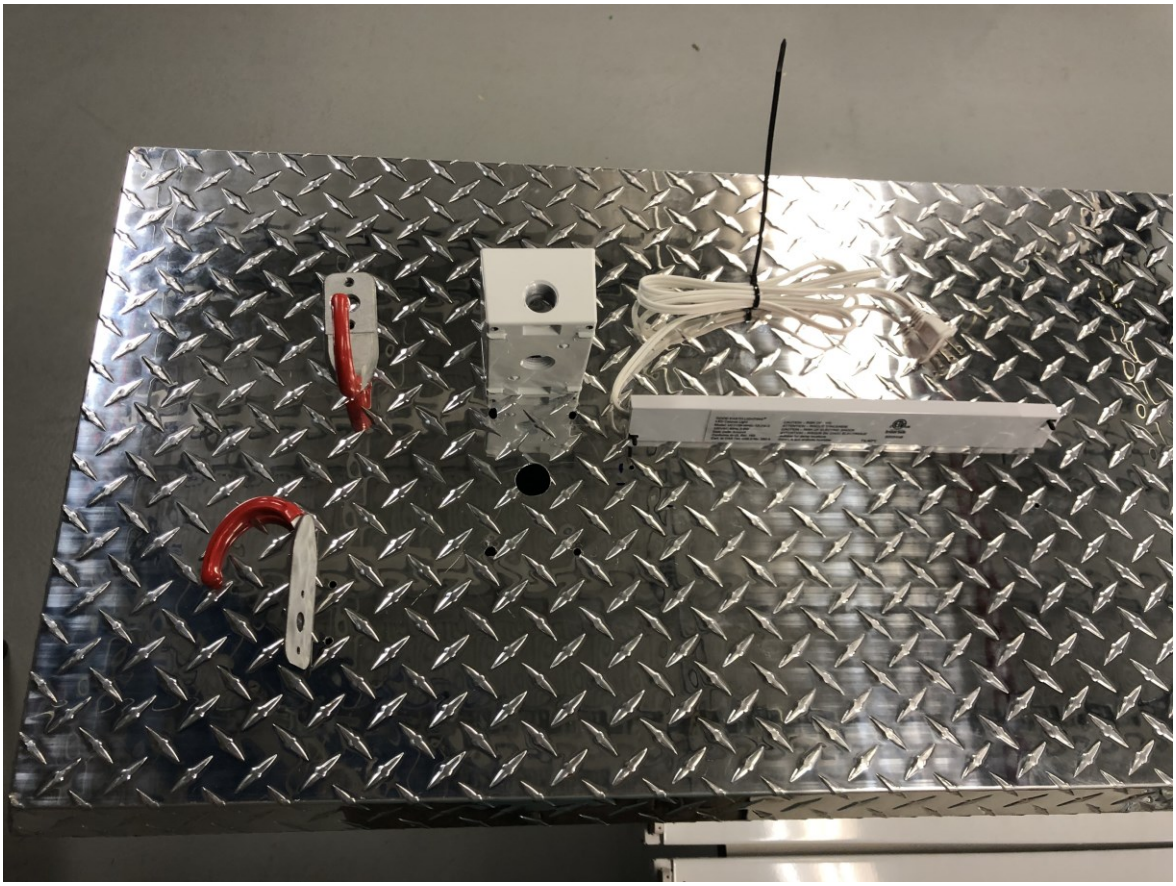

Figure B.3 The two J-hooks, the external switch box, and the LED strip light layout on top of the toolbox lid

11. Mount the two J-hooks and LED strip light with 10-32 bolts and lock nuts. Mount the external switch box with the 1/2” rigid comp connector as shown in Figure B.4.

Figure B.4 The external switch box mounted with the 1/2” rigid comp connector

12. Next, remove the left-hand hydraulic lift arm in the toolbox by using a flat-head screwdriver to pop the metal tabs on the top and bottom of the lift arm as shown in Figure B.5.

Figure B.5 The left-hand hydraulic lift arm in the toolbox

13. Using the stepper drill bit, drill four holes in the upper left hand sheet metal of the inner toolbox wall according to Figure B.6. Use the power strip's mounting holes as a template for the inner two holes. Fill the outer two holes with the two rubber grommets once drilled.

Figure B.6 The four mount holes drilled in the upper left-hand plate in the inside of the toolbox

14. Cut the cable of the power strip twice to form three sections with the wire cutters. The first section, moving from the strip to the plug, should be about 1-3/4’ long. The next middle section should be 2’ long. The third section is just what remains of the cable and should be about 12’ long.
15. Mount the power strip with 10-24 bolts and lock nuts and ensure that it is level. The end of the power strip where the power cable enters should be facing the front of the toolbox. This is shown in Figure B.7.

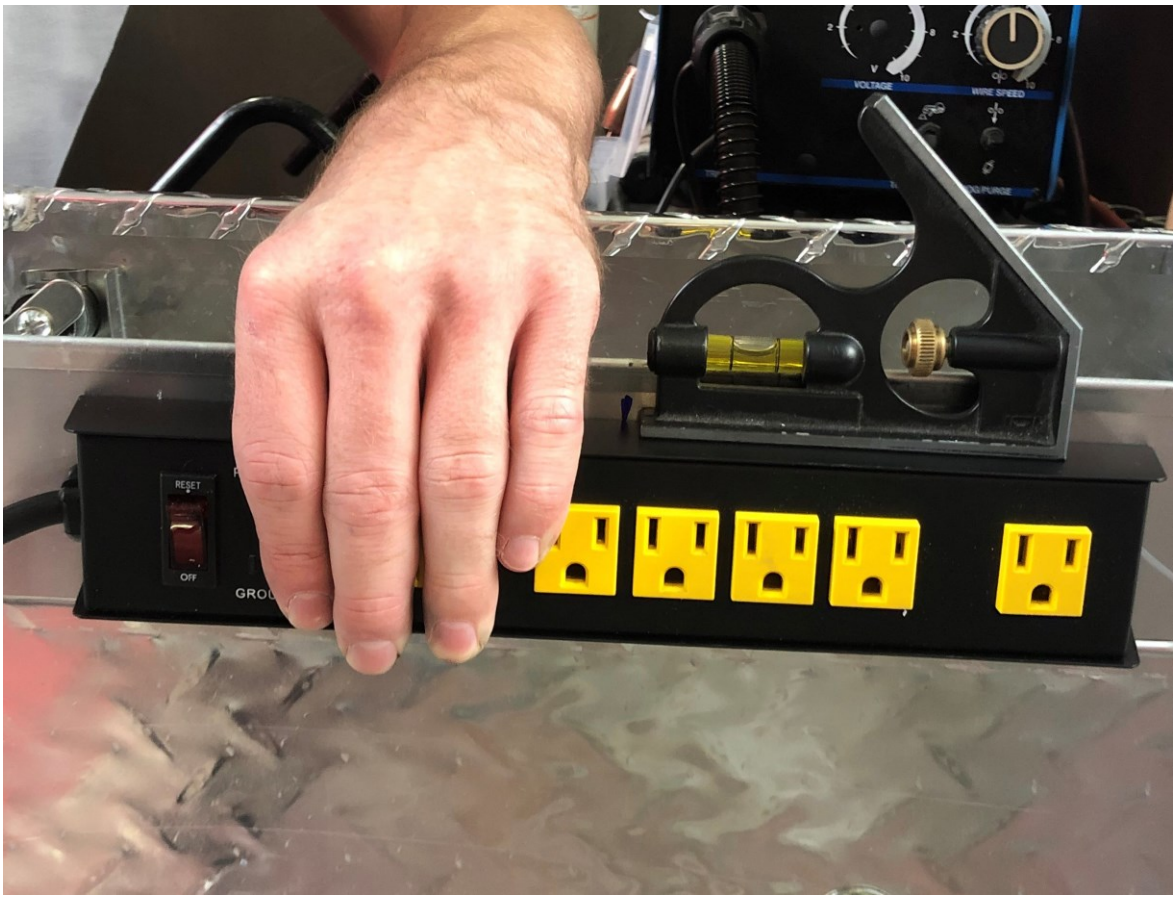

Figure B.7 The leveled power strip with the power cord facing the front of the toolbox

16. With the power strip mounted, feed the power through the grommeted hole closest to the front of the toolbox as shown in Figure B.8.

Figure B.8 The power cable of the power strip fed through the grommeted hole closest to the front of the toolbox

17. Cut the power cable of the LED strip light 1’ from the plug and feed it through the hole in the external switch box that faces the back of the toolbox. Then, feed the cable through the bottom hole of the external switch box and down into the toolbox.
18. Now, drill two holes in the RACO internal switchbox – one in the bottom small side and one in the top small side. The bottom hole should be a 1/4” in diameter, and the top hole should be just barely bigger than the threads of the 15A contact switch. These holes can be seen in Figure B.9.

Figure B.9 The 1/4” hole in the bottom and the contact switch hole in the top of the RACO internal switch box

19. Punch out the center metal disk on the righthand side of the RACO internal switch box. Then, punch out the center metal disk of the RACO internal switch box cover. Both holes are shown in Figure B.10. Put large rubber grommets in both the middle hold of the internal switch box and the switch box cover.

Figure B.10 The side and front cover punched out holes in the RACO internal switch box and cover

20. Using the hand drill, drill a hole in the floor of the upper left-hand side of the toolbox 1/4” in diameter.
21. Mount the RACO internal switch box to the toolbox in the upper left-hand side using a 1/4” bolt and lock nut with the open side of the internal switch box facing the front of the toolbox as shown in Figure B.11.

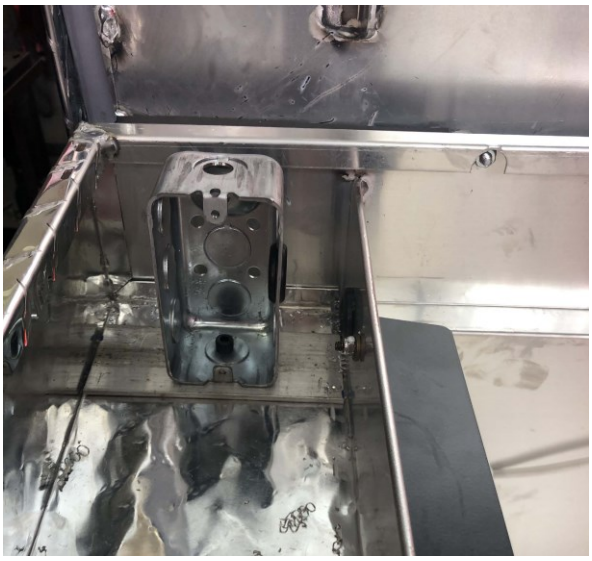

Figure B.11 Mounted RACO internal switch box facing the front of the toolbox

22. Measure the length of the inner front wall of the toolbox and make a mark at the halfway point.
23. Measure 1/2” off the floor of the toolbox on the left-hand side looking of the centerline and make a mark.
24. Align the workhorse ballast with these two marks so that the edge of the ballast with the red wires is aligned with the centerline of the toolbox marked in step 22, the bottom of the ballast is aligned with the mark made in step 23, and the black and white wires are pointed towards the side of the toolbox with the power strip as shown in Figure B.12.

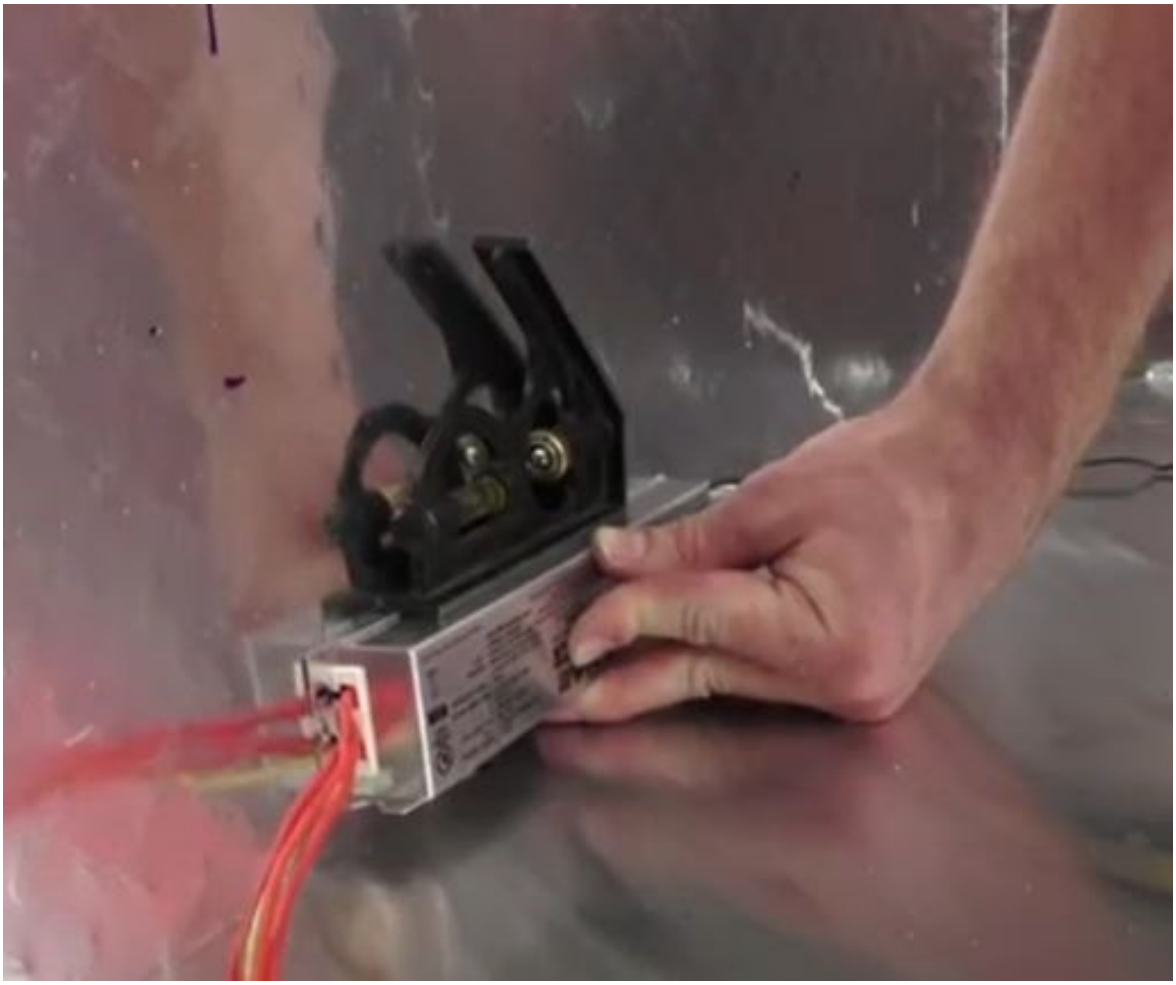

Figure B.12 Leveled workhorse ballast in mount location

25. Ensuring that the ballast is level, mark the mount holes and drill the mount holes.

26. Mount the ballast with 10-32 bolts and lock nuts.

27. Take the middle cover off each of the 36” fluorescent light fixtures and remove the ballast, shown in Figure B.13, that comes in the fixtures.

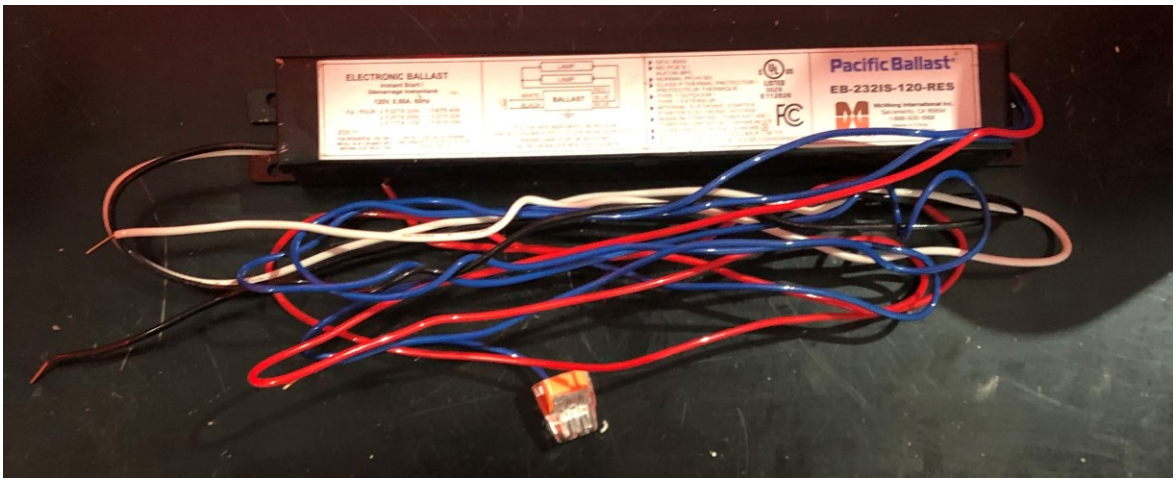

Figure B.13 Discarded ballast example from inside the fluorescent light fixture

28. Now, measure the center height and center width of both the inner front and back walls of the toolbox, and make crosses at their intersection.
29. Align one of the fluorescent light fixtures on the back wall so that it is level, and its center point matches the center point marked in step 28. This is shown in Figure B.14. Mark the mount holes.

Figure B.14 Fluorescent light fixture leveled and in mount location

30. Drill the mount holes and mount the fixture with 1/4” bolts.
31. Repeat steps 29-30 for the front wall of the toolbox and mount the second fixture.
32. Next following the diagram shown in Figure B.15, wire the workhorse ballast to the two fluorescent light fixtures.

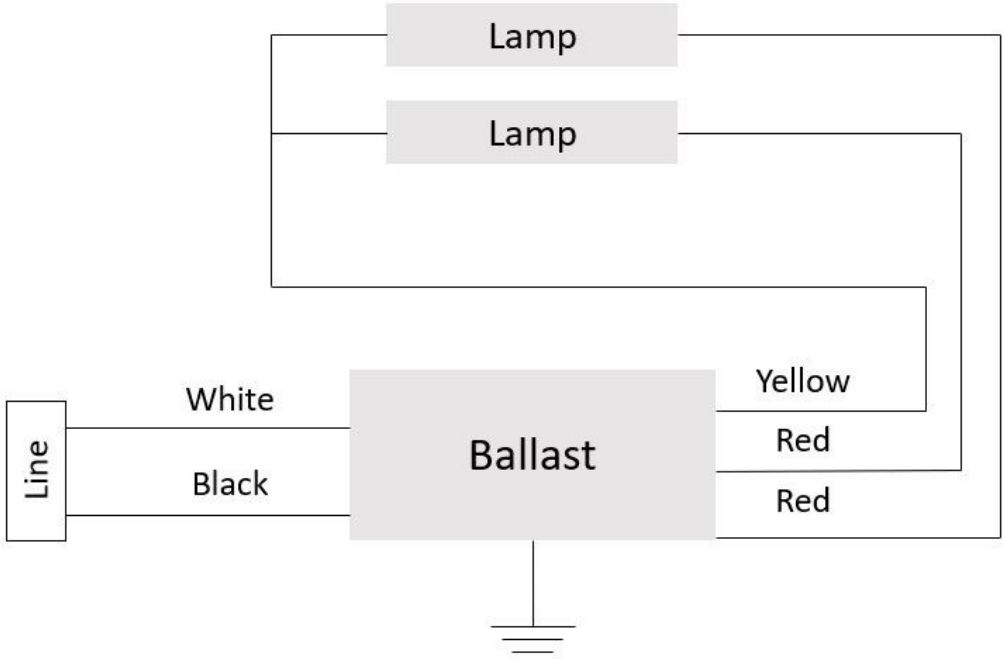

Figure B.15 The wiring diagram for the workhorse ballast and the two fluorescent light fixtures

33. Close the lid and feed the wire end of the 12’ long section of the power strip’s cable through the hole of the external switch box that faces the back of the toolbox.
34. Wire the 12’ long, plug end of the power strip’s cable to the dial timer, and wire one end of the 2’ length of the power strip’s cable from the dial timer and into the box as shown in Figure B.16. NOTE: When wiring, wire the white wire of each cable to one another; wire the green wire of each cable and the copper lead of the dial timer to each other, and wire one black wire into one end of the dial timer and the other black wire into the other end of the dial timer.

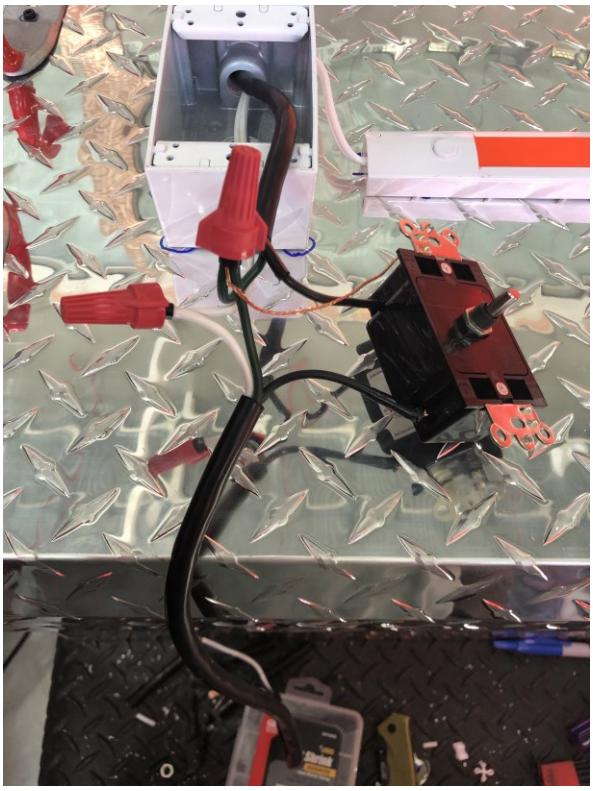

Figure B.16 The wiring of the 12’ and 2’ lengths of the power cable to the dial timer

35. Feed the other end of the 2’ long section of the power strip’s cable through the bottom of the external switch box and down into the toolbox.
36. With the dial timer wired, use 10-32 bolts to mount the dial timer to the external switch box as shown in Figure B.17.

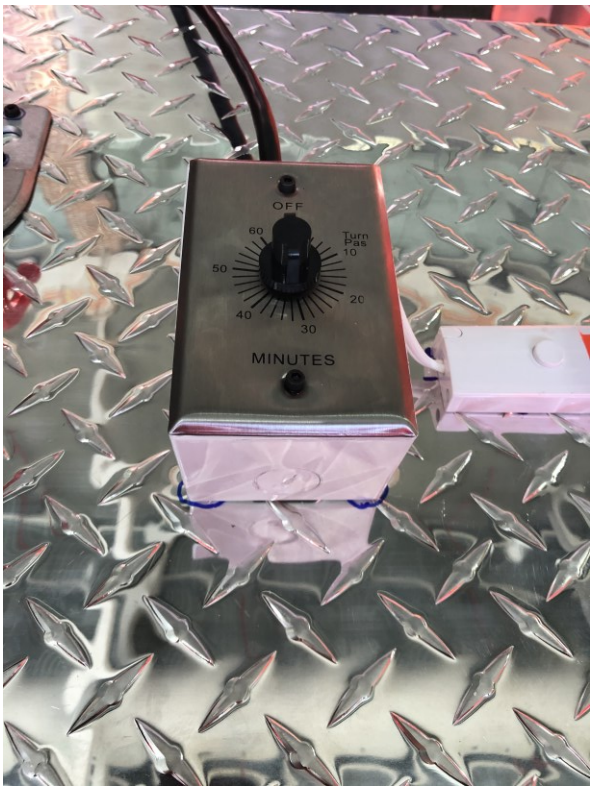

Figure B.17 The dial timer mounted into the external switch box once wired with 10-32 bolts

37. Take the 12’ section of the power strip’s cable that exits the external switchbox and wrap it once around the two J-hooks to the left of the external switch box. Zip-tie the wrap to itself twice to create a strain relief for the power cable as shown in Figure B.18.

Figure B.18 The strain relief of the power cable on the J-hooks with zip-ties

38. Open the lid and feed the 2’ long section of the power strip’s cable through the rubber grommeted hole closest to the back of the toolbox and through the rubber grommeted hole of the RACO internal switch box.
39. Wire this end of the 2’ long section of the power strip’s cable to the 15A contact switch and to the end of the power cable coming from the power strip. Feed the end of the power strip cable still attached to the power strip through the grommeted hole in the RACO internal switch box cover prior to wiring. NOTE: Wire the green wire of the 2’ section to the green wire of the 1-3/4’ section. Similarly, wire the white to the white, and then wire each black wire to a crimp spade connector. Push each crimp spade connector once wired onto the leads of the 15A contact switch. The wired assembly is shown in Figure B.19.

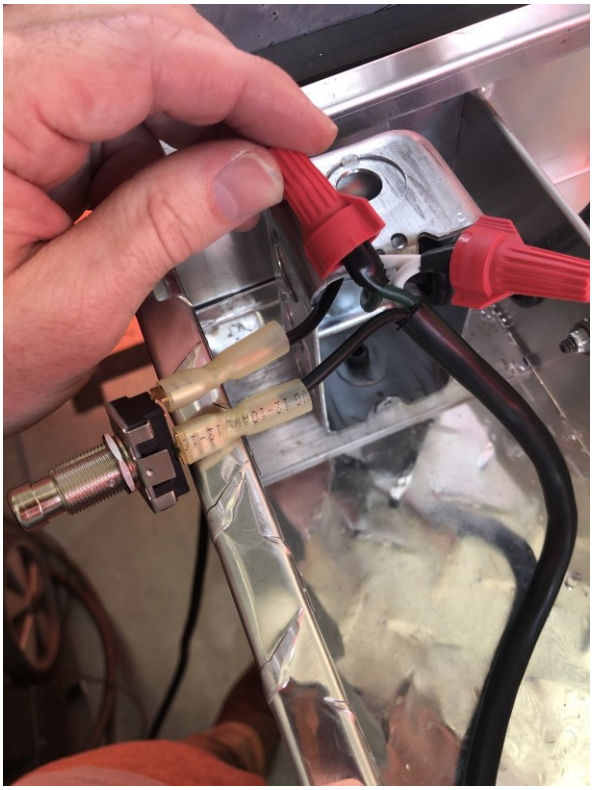

Figure B.19 The wiring of the 2’ length of power cable and the power strip to the 15A contact switch

40. Install the wired assembly into the RACO internal switchbox by feeding the 15A contact switch up through the hole in the top of the internal switch box. Place the thin nuts that come with the contact switch such that the very top of the contact switch is 1/4” above the top of the internal switchbox. This is shown in Figure B.20.

Figure B.20 The wired 15A contact switch mounted into the RACO internal switch box

41. Now, test the power system. Do this by plugging in the power cable mounted to the J-hooks to a wall outlet, turning the dial timer past 10 minutes, and holding down the contact switch. Ensure the breaker is flipped up on the power strip which will make the indicator lights on the power strip come on. If this happens, then the power system is working.
42. Mount the RACO internal switch box cover to the RACO internal switch box with the screws supplied with the switch box as shown in Figure B.21.

Figure B.21 The RACO internal switch box cover shown mounted to the RACO internal switch box

43. Wire the plug end of the LED strip light's power cable back to the end of the cable that is still connected to the strip light. Make sure that the end attached to the strip light is still fed through the hole of the external switch box closest to the back of the toolbox and down through the bottom hole into the toolbox. Once the LED strip light's power cable is wired back together, plug the plug end into the power strip inside the toolbox as shown in Figure B.22.

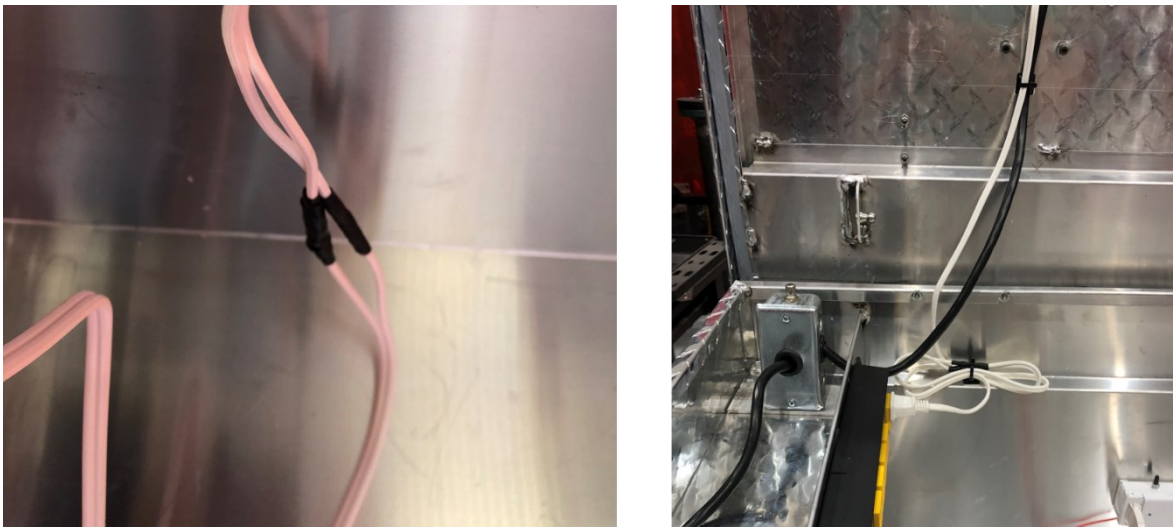

Figure B.22 The LED strip light power cable wired back together and plugged in to the power strip

44. Repeat the power test of the toolbox, but this time make sure that the LED strip light turns on. If it does not, press the small white button on the strip light. If it still does not come on, then there is an issue with the wiring. Once the light is functioning with the rest of the toolbox **DO NOT touch the white button again** as this will disable the indicator light.
45. Now, cut 1-1/2’ of the 16-gauge power cable as measured from the plug end.
46. Wire the 16-gauge power cable to the black and white wires of the workhorse ballast. Wire the green cable to the mount point of the ballast to create a ground. The completed wiring harness is shown in Figure B.23.

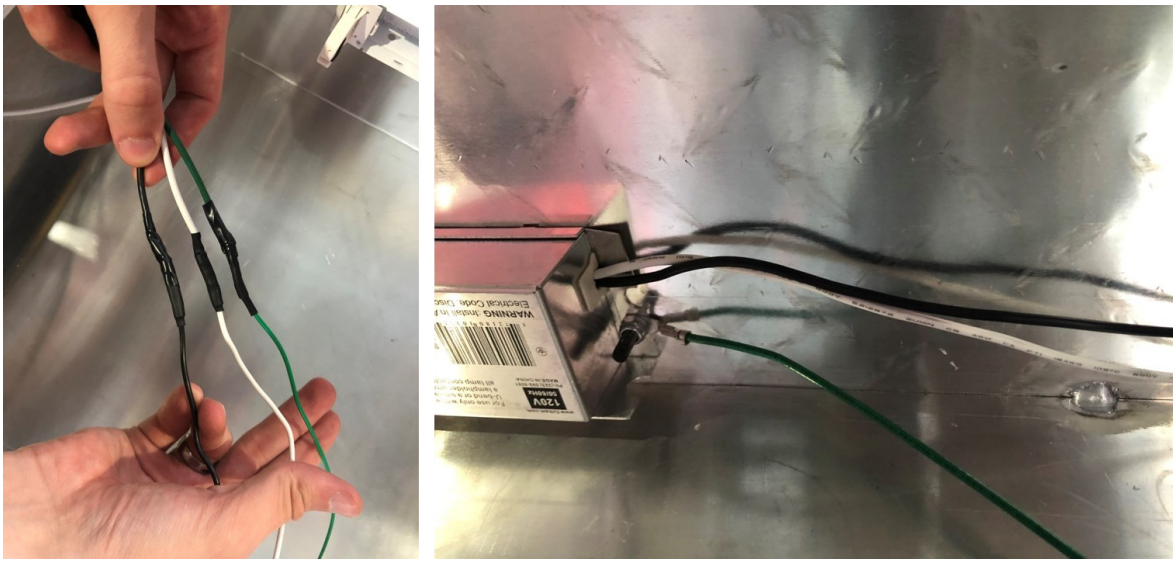

Figure B.23 The workhorse ballast wired to the 16-gauge power cable

47. Once wired, plug the 16-gauge power cable into the power strip.

48. Using 1/4” bolts and lock nuts, put 2 bolts in the top side of each end of each fluorescent fixture as shown in Figure B.24.

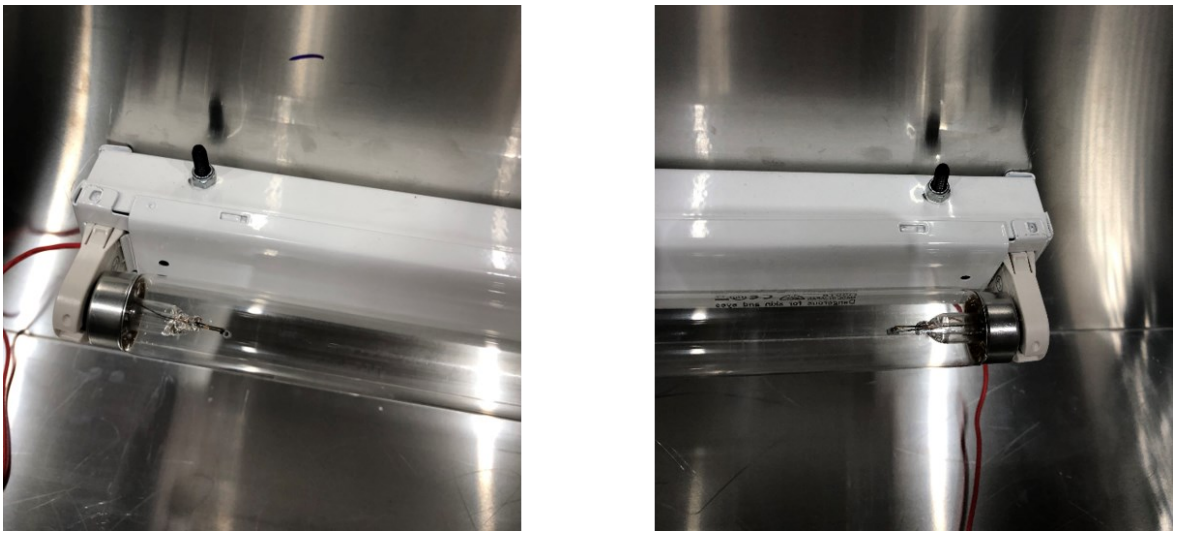

Figure B.24 The two 1/4” bolts and lock nuts in the top of both ends of the fluorescent light fixture

49. Replace the white covers over the fluorescent fixtures and install the G30T8 germicidal bulbs.
50. Cut the perforated aluminum into two sections 36” long and 11” wide each.
51. Once cut, use the sheet metal brake to bend each piece of perforated aluminum in three places along the 11” wide to create the geometry shown in Figure B.25. NOTE: if a sheet metal brake is unavailable, then pliers and a hammer can be used to shape the aluminum into roughly the same geometry.

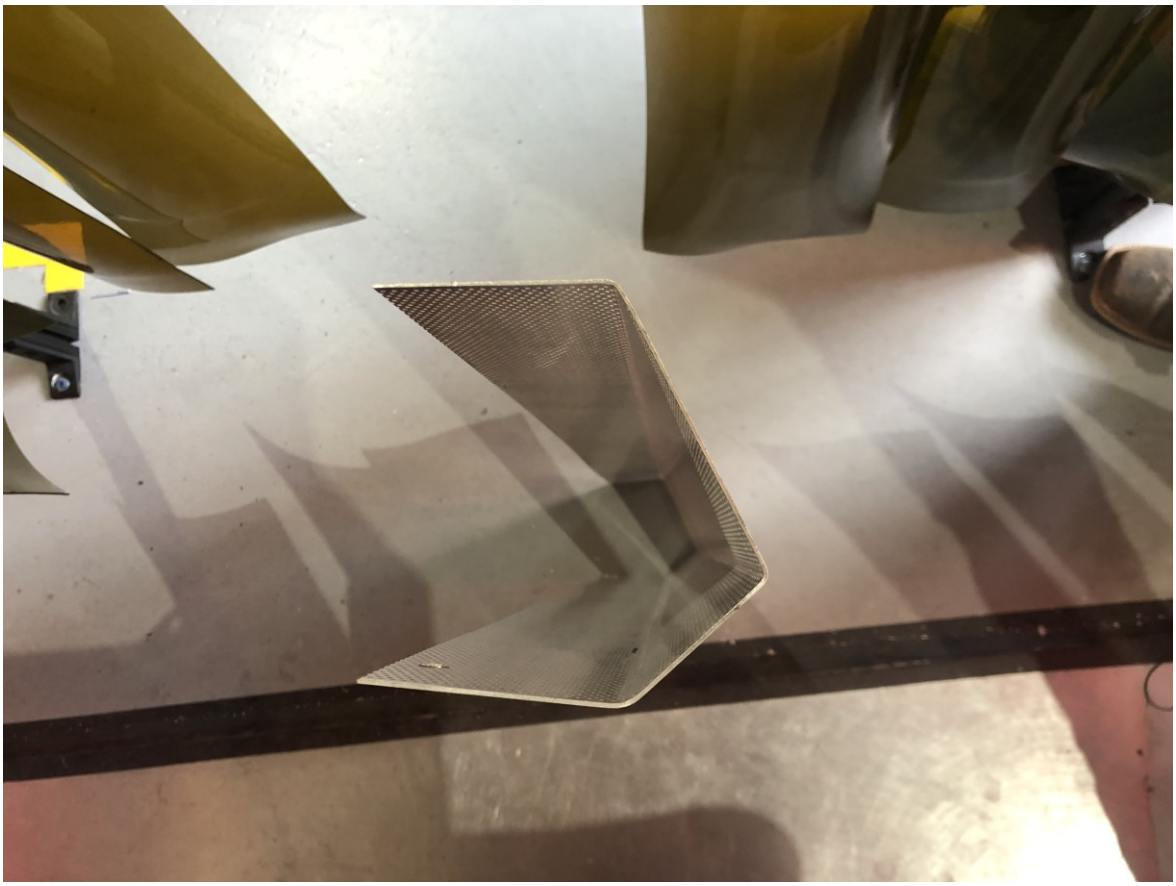

Figure B.25 The geometry of a completed aluminum covering

52. Drill a hole in each end of the top side of each of the perforated aluminum covers corresponding to the bolts in the tops of each of the two fluorescent fixtures. Make the holes larger than the 1/4” bolts.
53. Install the aluminum covers on the fluorescent fixtures onto the 1/4” bolts so that they cover the lights as shown in Figure B.26.

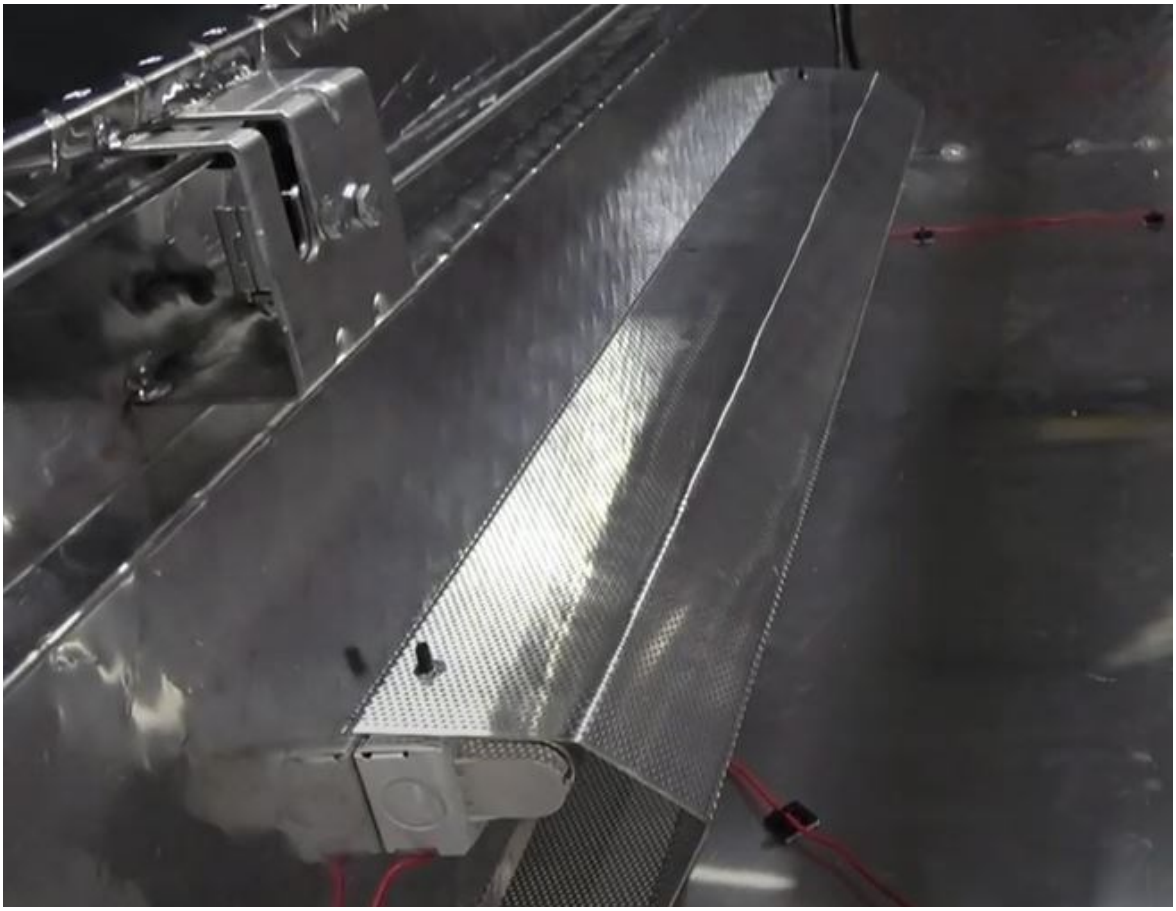

Figure B.26 An aluminum covering installed onto the fluorescent light fixture

54. Next, measure the center of each of the short walls and make a mark.
55. Then, measure 9” off the floor on each of the short walls and make a mark so that there is a cross mark on each short wall.
56. Using the hand drill, drill a hole in the center of each of the crosses 1/4” in diameter.
57. Measure and cut 5-1/2’ of the aluminum hanging wire.
58. Using 1/4” bolts, wrap each end of the aluminum wire once around the head of the bolts, then mount the bolts in the drilled hole with lock nuts so that the wire is pulled tight between them as shown in Figure B.27.

Figure B.27 The aluminum hanging wire mounted in the toolbox by the 1/4” bolts in each end

59. Once mounted, use the pliers to twist the wire gently to tighten as needed.

60. Close the lid and evenly space the two tow handles on the upper right-hand side of the toolbox so that they are centered as shown in Figure B.28.

Figure B.28 The tow handles leveled, spaced, and mounted onto the upper right-hand side of the toolbox

61. Using the screws supplied with the handles and the hand drill, mount the handles to the box.
62. Measure 1” in from either side and 1/4” up from the bottom, lower left-hand side of the toolbox, and make marks at both these locations.
63. Align the casters vertically so that they match the corners marked in the previous step and mark the mount holes.
64. Drill the four mount holes for each caster and mount each caster with 1/4” bolts and lock nuts as seen in Figure B.29.

Figure B.29 The casters leveled, aligned, and mounted on the lower left-hand side of the toolbox

65. Open the lid and vacuum out the metal shavings from inside the box.

66. Use the zip-ties and zip-tie holders to organize the power cables in the toolbox as shown in Figure B.30.

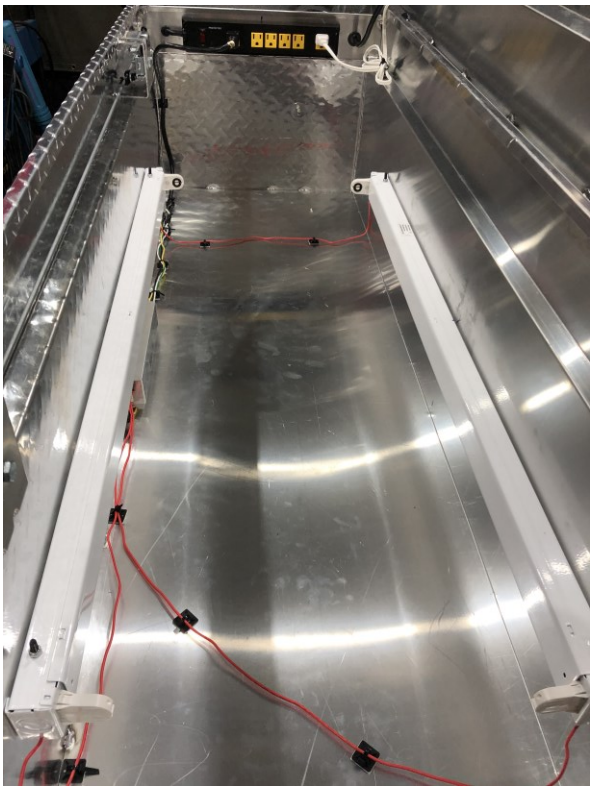

Figure B.30 The wiring harnesses for the fluorescent light fixtures, workhorse ballast, and LED strip light organized and mounted with the zip-ties and zip-tie holders

67. Using the white duct tape, tape across the width of the toolbox on the floor from one end of a fluorescent fixture to the same end of the opposite fluorescent fixture, thus creating a boundary at each end of the fluorescent fixtures as shown in Figure B.31.

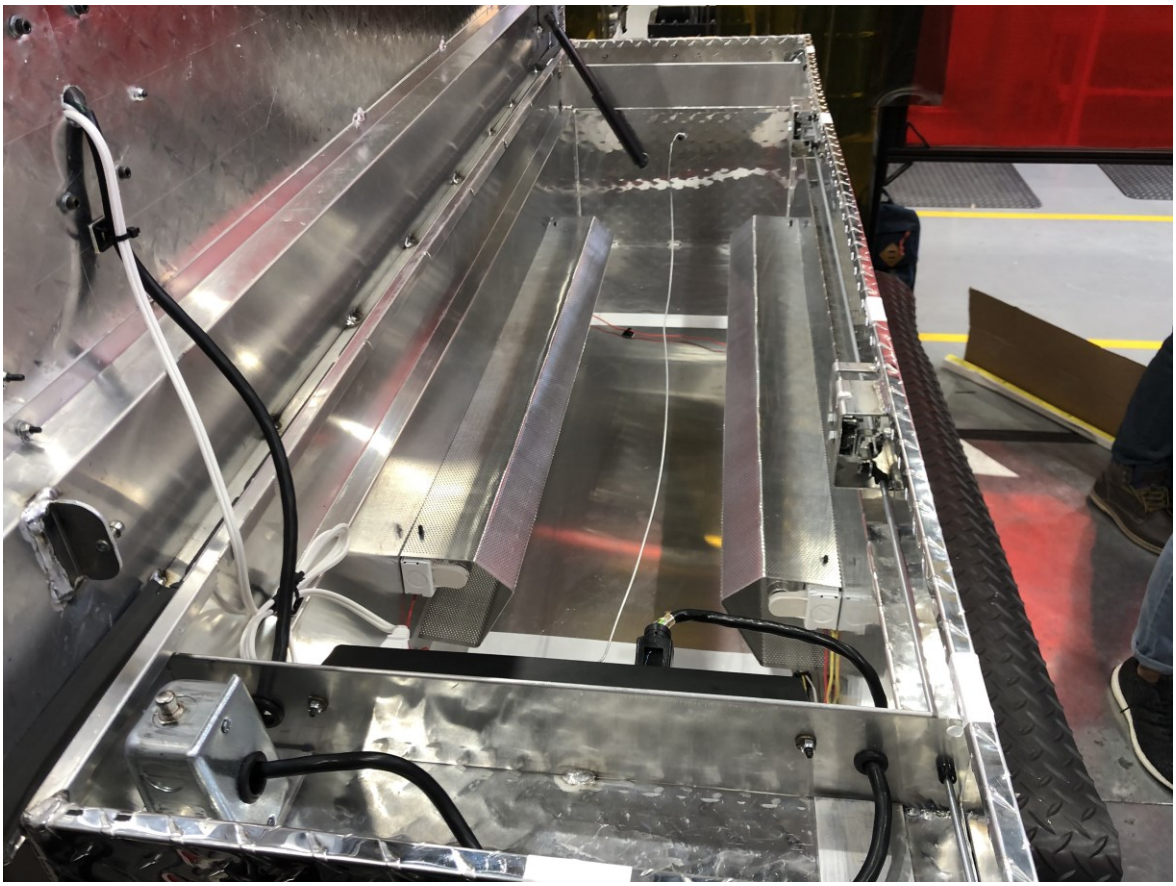

Figure B.31 The completed inside of the toolbox with the two white duct tape borders on the floor

68. Close the lid and tape off three rectangles with the white duct tape on the lid and upper part of the toolbox. The first rectangle should be over the front left corner of the toolbox. The second should be a 2’ long rectangle in the center, and the third should cover the whole upper right-hand side of the toolbox. These can be seen in Figure B.32.

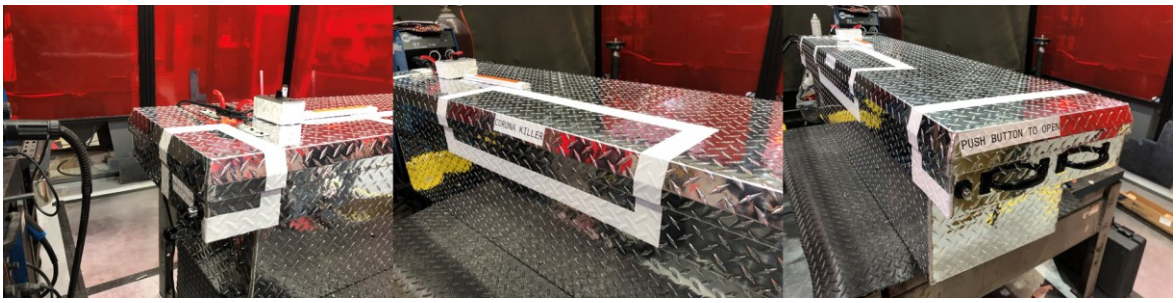

Figure B.32 The three rectangle sections on the outside of the toolbox denoted by the white duct tape

69. Once the taping is complete, it is optional to use a label marker to print operational instructions for the UVC disinfection chamber.

70. The UVC disinfection chamber is now complete and can be seen in Figure B.33.

Figure B.33 The completed UVC Disinfection Chamber on display